

# Vulnerability of C6 Astrocytoma Cells After Single-Compound and Joint Exposure to Type I and Type II Pyrethroid Insecticides

Delfina M. Romero,<sup>\*,†,‡,1</sup> Bruno G. Berardino,<sup>†,§</sup> Marcelo J. Wolansky,<sup>\*,†,‡,2,3</sup> and Mónica L. Kotler<sup>†,‡,¶,3</sup>

<sup>\*</sup>Laboratorio de Toxicología de Mezclas Químicas; <sup>†</sup>Departamento de Química Biológica, Facultad de Ciencias Exactas y Naturales, Universidad de Buenos Aires, Argentina; <sup>‡</sup>IQUIBICEN-Argentina National Research Council (CONICET); <sup>§</sup>Laboratorio de Neuroepigenética; and <sup>¶</sup>Laboratorio de Disfunción Celular en Enfermedades Neurodegenerativas y Nanomedicina

<sup>1</sup>Present address; Institut du Fer à Moulin, INSERM UMRS 839, Paris, France; Sorbonne Universités, Université Pierre et Marie Curie, Paris, France.

<sup>2</sup>To whom correspondence should be addressed at Laboratorio QB48, Piso 4, Pabellón 2, Ciudad Universitaria, Universidad de Buenos Aires, Ciudad Autónoma de Buenos Aires (1428EGA), Argentina. Fax: 541145763342. E-mail: mjwolansky@qb.fcen.uba.ar.

<sup>3</sup>These authors contributed equally to this study.

## ABSTRACT

A primary mode-of-action of all pyrethroid insecticides (PYRs) is the disruption of the voltage-gated sodium channel electrophysiology in neurons of target pests and nontarget species. The neurological actions of PYRs on non-neuronal cells of the nervous system remain poorly investigated. In the present work, we used C6 astrocytoma cells to study PYR actions (0.1–50  $\mu\text{M}$ ) under the hypothesis that glial cells may be targeted by and vulnerable to PYRs. To this end, we characterized the effects of bifenthrin (BF), tefluthrin (TF),  $\alpha$ -cypermethrin ( $\alpha$ -CYP), and deltamethrin (DM) on the integrity of nuclear, mitochondrial, and lysosomal compartments. In general, 24- to 48-h exposures produced concentration-related impairment of cell viability. In single-compound, 24-h exposure experiments, effective concentration ( $\text{EC}_{15}$ )<sub>S</sub> 3-(4,5-dimethyl-thiazol-2-yl)-2,5-diphenyl-tetrazolium bromide (MTT assay) were computed as follows (in  $\mu\text{M}$ ): BF, 16.1; TF, 37.3;  $\alpha$ -CYP, 7.8; DM, 5.0. We found concentration-related damage in several C6-cell subcellular compartments (mitochondria, nuclei, and lysosomes) at  $\geq 10^{-1}$   $\mu\text{M}$  levels. Last, we examined a mixture of all PYRs (ie,  $\Sigma$  individual  $\text{EC}_{15}$ ) using MTT assays and subcellular analyses. Our findings indicate that C6 cells are responsive to nM levels of PYRs, suggesting that astroglial susceptibility may contribute to the low-dose neurological effects caused by these insecticides. This research further suggests that C6 cells may provide relevant information as a screening platform for pesticide mixtures targeting nervous system cells by expected and unexpected toxicogenic pathways potentially contributing to clinical neurotoxicity.

**Key words:** C6 cells; pyrethroids; cellular damage; cell death.

Whether simultaneous low-level exposure to multiple pesticides may be a potential etiological factor of nervous system disorders is still under debate (Carpy *et al.*, 2000; Hernández *et al.*, 2013; McManus *et al.*, 2013). In general, toxicological studies considered to establish safe pesticide exposure levels often use testing conditions based on the available evidence of the mode-of-action (MOA) and dose-response assays in laboratory animals administered a few

doses of a single compound to estimate reference doses, ie, threshold dose levels above which toxicity may be expected in susceptible individuals (Izadi *et al.*, 2012; USEPA, 2002). Regulatory study designs “blind” to “secondary” target sites may be expected to contribute to the overall health risk uncertainty, especially when members of a pesticide class such as pyrethroids (PYRs) present toxicological divergence (Wolansky and Harrill, 2008).

PYRs are synthetic insecticides increasingly used in home and agricultural pest control (Krieger, 2010). Low levels of PYR residues are present in water streams, soil, air, food, homes, human urine, and breast milk (CDC, 2015; Corcellas et al., 2012; FDA, 2015; Morgan, 2012; Tolve et al., 2006; Wielgomas et al., 2013). PYRs have been historically classified into subclasses as follows: type I compounds, which do not contain an  $\alpha$ -cyano group, and type II compounds, which do contain this group. In general, type-I PYRs induce T-syndromes in small rodents, characterized mainly for the presence of tremors, whereas type-II PYRs induce CS-syndromes, causing choreoathetosis and salivation. There are also a few PYRs classified as mixed-type I/II, which produce a TS-syndrome, causing tremors and salivation (Wolansky and Harrill, 2008).

PYRs may produce intense electrophysiological alterations in targeted neurons in the nervous system, supporting the general classification of these insecticides as neurotoxicants (Soderlund et al., 2002). Most of the research conducted during the last decades has explored the clinical manifestations resulting from the disruption of neuronal voltage-gated sodium channel (VGSC) conductance, proposed to be central to the mechanism of PYR toxicity in mammals (Narahashi et al., 2007; Soderlund et al., 2002). However, evidence for alternative target sites, including pharmacological actions of several cyano-PYRs in the GABAergic system, electrophysiological changes in other voltage-gated ion channels, and modulation of neurotransmitter release or uptake rates, has been generated (Crofton and Reiter, 1987; Krieger, 2010; Shafer and Meyer, 2004; Soderlund, 2012; Soderlund et al., 2002). Moreover, PYRs can cause endocrine disruption, reduction in beating frequency and amplitude in cultures of cardiac myocytes, inhibition of spontaneous glutamate network-dependent spikes and bursts in primary cultures of neurons, liver tumors, and teratogenic effects in the rat (Go et al., 1999; Koureas et al., 2012; Natarajan et al., 2006; Osimitz and Lake, 2009; Pine et al., 2008; Shafer et al., 2008; Tsuji et al., 2012).

Data on neurological effects in laboratory animals is not sufficient to ascertain the vulnerability of glia-related cells after low-dose exposure to PYRs. Astrocytes constitute approximately 50% of the brain tissue and actively participate in physiological mechanisms required to maintain normal conditions in neurons, including glutamate reuptake in the synaptic junction, glutamine release, and  $K^+$  and  $H^+$  buffering (Sofroniew and Vinters, 2010). Some *in vivo* studies in adult rats have shown that PYRs may damage brain astroglia in addition to targeting neurons. Malkiewicz et al. (2006) found a decrease in Glial fibrillary acidic protein (GFAP) immunoreactivity without any evident change in the number or morphology of astrocytes in several brain regions a few weeks after 6-day oral exposure to low-effective doses of cypermethrin (CYP), whereas Tayebati et al. (2009) reported increased number and size of GFAP-immunoreactive cells in cortical and hippocampal regions after a dermal exposure scheme simulating a maximal occupational exposure to the same PYR for 4 weeks. In addition, Abdel-Rahman et al. (2001) found that a low-dose dermal exposure to permethrin prolonged for 60 days caused multiple alterations in the central nervous system, including neuronal cell death and astrocyte hypertrophy in the hippocampus and cerebellum. Mense et al. (2006) observed that exposure to  $10^0$ – $10^2$   $\mu$ M concentrations of another PYR, Cyfluthrin, for 7–14 days caused alterations in cell culture growth and various functional markers of human fetal astrocytes. These authors found that while lactate dehydrogenase release and glutamate uptake assays showed astrocyte susceptibility starting at

low  $\mu$ M levels, the cell number was reduced only at concentrations  $\geq 25$   $\mu$ M and activation of apoptosis-related factors were observed at 50–100  $\mu$ M. Furthermore, in the rat brain astroglia-derived C6 cell line, Culliford et al. (2004) reported that cyano- and noncyano-PYRs altered ion and organic osmolyte trafficking phenomena in the plasma membrane and cell volume-related signaling processes after exposure to 100  $\mu$ M. Last, Maurya et al. (2012) assessed the developmental neurotoxicity of CYP after 2-week oral exposure (10–25 mg/kg as a daily dose) in infant rats and also examined primary cultures of rat brain astrocytes after exposure for 24–48 h to this compound (50–200  $\mu$ M). These CYP studies showed increased rates of apoptosis in cerebral cortex astrocytes. In general, these previous studies did not test a representative selection of cyano- and noncyano-PYRs using a glia-derived cell culture under comparable experimental conditions. Moreover, PYR-induced alterations *in vivo* and *in vitro* were observed after using excessive exposure schemes as compared with the expected environmental levels in the general population (CDC, 2015; FDA, 2015; Morgan, 2012; Tolve et al., 2006). Most importantly, a relevant question that remains to be determined is the threshold concentration at which PYRs may damage astroglia-related cell types, potentially weakening glial mechanisms that contribute to optimal neuronal function.

The aim of the present work was to characterize the toxicological effects of individual PYRs and a quaternary mixture in C6 cells, using a comprehensive battery of biochemical and subcellular markers and extensive time-concentration-effect schemes. C6 cells keep many physiological features of astrocytes and have been extensively used to characterize pharmacological and toxicological responses to neuroactive substances (Alaimo et al., 2011; Benda et al., 1968; Cookson et al., 1995; Posada-Duque et al., 2015). The interaction between glial cells and neurons has been demonstrated to exert a major influence on the structural arrangement and functional output of neuronal circuits under physiological and pathological conditions (Lee et al., 2014; Zeidán-Chuliá et al., 2014). We found that C6 cells are vulnerable to nM levels of types I and II PYRs. In addition, the multiple subcellular anomalies observed at nM– $\mu$ M levels imply that toxicogenic pathways unrelated to the primary MOA described in neurons were sensitive and reactive to PYRs.

## MATERIALS AND METHODS

**Reagents.** Dulbecco's Modified Eagle's Medium (DMEM), 3-(4,5-dimethyl-thiazol-2-yl)-2,5-diphenyl-tetrazolium bromide (MTT), 3-Amino-7-dimethylamino-2-methylphenazine hydrochloride (neutral red [NR]), and 2'-(4-Hydroxyphenyl)-5-(4-methyl-1-piperazinyl)-2,5'-bi(1H-benzimidazole) trihydrochloride (Hoechst-33258 fluorochrome) were purchased at Sigma Chemical Co (St Louis, Missouri). 1H,5H,11H,15H-Xantheno[2,3,4-ij:5,6,7-i'j']diquinolizin-18-ium, 9-[4-(chloromethyl)phenyl]-2,3,6,7,12,13,16,17-octahydrochloride 167095-09-2 (MitoTracker Red CMXRos), and (3-{2-[(1H,1'H-2,2'-bipyrrrol-5-yl-kappaN(1))methylidene]-2H-pyrrol-5-yl-kappaN)-N-[2-(dimethylamino)ethyl]propanamido) (difluoro boron) (LysoTracker Red DND-99) were from Invitrogen, Thermo Fisher Scientific Inc. Fetal bovine serum (FBS) was obtained from Natocor (Córdoba, Argentina). N-(2-hydroxyethyl) piperazine-NO-(2-ethanesulfonic acid) (HEPES) was from ICN Biomedicals (Irvine, California). Technical grade samples of 4 PYR insecticides were examined in this work. Tefluthrin (TF, 3-(2-chloro-3,3,3-trifluoropropenyl)-2,2-dimethyl-cyclopropanecarboxylic acid tetrafluoromethyl-benzyl ester; Product Code IC1993 technical, purity 96.3%) was kindly provided by its manufacturer, Syngenta (Greensboro,

North Carolina). Deltamethrin (DM, (S)- $\alpha$ -cyano-3-phenoxybenzyl (1R)-cis-3-(2,2-dibromovinyl)-2,2-dimethylcyclopropanecarboxylate, Catalog No. PS-2071, purity 99.5%), a racemic mixture of bifenthrin (BF, 2-methylbiphenyl-3-ylmethyl (Z)-(1R,3R)-3-(2-chloro-3,3,3-trifluoroprop-1-enyl)-2,2-dimethylcyclopropanecarboxylate, Catalog No. PS-2003, purity 99.0%), and  $\alpha$ -cypermethrin ( $\alpha$ -CYP, [racemate comprising (R)- $\alpha$ -cyano-3-phenoxybenzyl (1S)-cis-3-(2,2-dichlorovinyl)-2,2-dimethylcyclopropanecarboxylate and (S)- $\alpha$ -cyano-3-phenoxybenzyl (1R)-cis-3-(2,2-dichlorovinyl)-2,2-dimethylcyclopropanecarboxylate; Catalog No. PS-2083, purity 99.5%) were purchased from ChemService, Inc (West Chester, Pennsylvania). A detailed toxicological classification of the test compounds may be obtained from Soderlund *et al.* (2002) and Wolansky and Harill (2008). Figure 1 shows the chemical structures of the PYRs examined.

**Cell culture.** The rat C6-ATCC CCL-107 cell line was kindly provided by Dr Zvi Vogel (Weizmann Institute of Science, Rehovot, Israel). C6 cells are derived from a cerebral astrocytoma originally induced by exposure of Wistar-Furth rats to N,N'-nitro-methyl-urea (Benda *et al.*, 1968). C6 cells were maintained in DMEM supplemented with 10% heat-inactivated FBS, 2.0 mM glutamine, 100 units/ml penicillin, 100  $\mu$ g/ml streptomycin, and 2.5  $\mu$ g/ml amphotericin B (Richet SA, Buenos Aires, Argentina).

Cells were cultured at 37°C in a humidified atmosphere of 5% CO<sub>2</sub> to 95% air.

The medium was renewed 3 times a week. For all experiments, C6 cells were removed with 0.25% trypsin, diluted with DMEM 10% heat-inactivated FBS, and replated into 12-well plates ( $1.5 \times 10^5$  cells/well), 96-well plates ( $2 \times 10^4$  cells/well), or 20 cm<sup>2</sup> plate ( $2 \times 10^5$  cells/plate) to yield 70% confluent cultures after 24 h (48 h in 20 cm<sup>2</sup> plates). Then, cells were washed with PBS. A battery of biochemical and morphological analyses were carried out in C6 cells (see later). Three independent experiments were conducted, and experimental results are expressed as percent change observed after each treatment compared with control (mean  $\pm$  SEM).

**Assessment of cell viability by the MTT assay.** The MTT assay was carried out to evaluate cell viability according to the protocol previously described (Mosmann, 1983) with slight modifications (Gonzalez *et al.*, 2008). The MTT test is considered a sensitive procedure to inform on mitochondrial energy metabolism and structural integrity (Mosmann, 1983). Briefly, cell cultures were prepared in 96-well plates and exposed to PYRs (type-II like  $\alpha$ -CYP and DM; type-I like BF and TF) for 4, 12, 24, and 48 h dissolved in 0.1% vol/vol dimethylsulfoxide (DMSO) vehicle in DMEM supplemented with 2% or 10% FBS. We further examined a quaternary

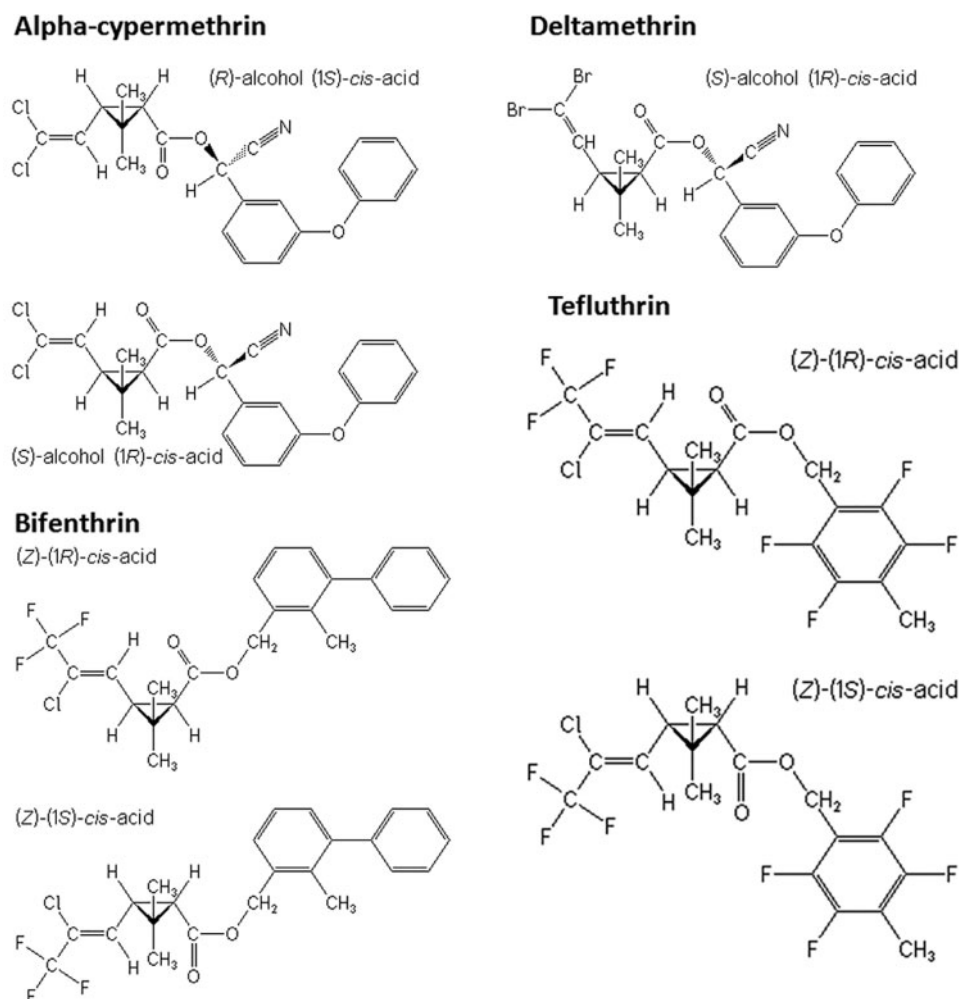


FIG. 1. Molecular structures of the 4 pyrethroid (PYR) compounds studied. Source: <http://www.alanwood.net/pesticides/index.html>.

mixture. The stock mixture comprised effective concentration (EC)<sub>15</sub> levels of all single compounds (EC<sub>15</sub> = concentration that causes a 15% decrease in response compared with vehicle-control cultures in 24-h exposure assays). Solutions were stirred and gently heated (approximately 40°C) to assure full solubility in cell culture medium. In the general population, taking into consideration environmental data (Morgan, 2012; Tulve et al., 2006; Wielgomas et al., 2013) and an efficient metabolism in mammals (Soderlund et al., 2002), levels of PYRs higher than 10<sup>2</sup> μM seem to be hardly plausible in target tissues. Accordingly, the final concentration of test chemicals in the culture medium ranged from 0.01 to 50 μM. The culture medium was removed after exposure. Cells were then washed twice with PBS pH 7.4, and 0.125 mg/ml of the MTT solution was added. After 2 h incubation, the reaction was stopped by addition of 200 μl DMSO/well. The MTT assay product was determined by measuring the absorbance at λ<sub>570 nm</sub> with background subtraction at λ<sub>655 nm</sub> in a Model 680 Benchmark microplate reader (BIO-RAD).

**Assessment of cell viability by the NR assay.** The NR assay was carried out following the protocol described by Alaimo et al. (2011). This cytotoxicity test is based on the ability of viable cells to incorporate the supravital dye NR in the conserved lysosomes. Following exposure for 24 h in DMEM supplemented with 2% FBS, cells were washed with PBS, and NR solution (50 μg/ml in DMEM) was added to each well. After 2 h incubation at 37°C, cells were first washed with PBS, and 200 μl of 50% ethanol/1% acetic acid solution was then added until complete dissolution. Absorbance was measured at λ<sub>570 nm</sub> with background subtraction at λ<sub>690 nm</sub> in a Model 680 Benchmark microplate reader.

**Cell morphology.** C6 cells (6 × 10<sup>4</sup> cells/well) were grown on glass coverslips in 12-well plates. After exposure to PYRs for 24 h cells were washed twice with PBS and fixed with 4% paraformaldehyde/4% sucrose (PFA-S) in PBS for 20 min at room temperature (RT). Finally, cells were washed with PBS and mounted on glass slides. Cell morphology was evaluated using differential interference contrast (DIC) and bright field microscopy. Samples were examined using a Leica microscope (Reichert Polyvar, Austria). Total cell area was determined based on DIC pictures using the ImageJ software (Research Services Branch, National Institute of Health [NIH]). Fifty cells were counted for each concentration evaluated. The average cell area value was expressed as % control ± SEM.

**Analysis of mitochondrial membrane integrity and nuclear morphology by fluorescence microscopy.** The mitochondrial morphology and membrane potential (Δψ<sub>m</sub>) dissipation were analyzed

according to Alaimo et al. (2014) by using MitoTracker Red CMXRos. This fluorochrome has been used to characterize physiological and chemical-induced programmed cell death processes involving structural and functional disruption of the mitochondrial network and oxidative stress (Gómez et al., 2007; Indo et al., 2007; Poot et al., 1997). Briefly, C6 cells (6 × 10<sup>4</sup> cells/well) were grown on glass cover slips in 12-well plates. After 24-h exposure to EC<sub>15/10</sub>, EC<sub>15</sub>, and EC<sub>30/max</sub> levels of single-compound or mixture dilutions, as previously estimated in the MTT assays (Table 1), cells were washed twice with PBS. The cultures were then incubated with a live cell permeant, mitochondria-specific red fluorescent probe, MitoTracker Red CMXRos (λ<sub>ex</sub>: 544 nm; λ<sub>em</sub>: 570 nm) at a final concentration of 35 nM in serum-free culture medium for 30 min at 37°C. After incubation, the cells were washed with PBS and fixed with PFA-S in PBS for 20 min at RT. The mitochondrial morphology was scored and classified according to Alaimo et al. (2011) as tubular (ie, +90% observations in DMSO-exposed control cultures), intermediate (ie, tubular mitochondria with swollen regions), and fragmented (ie, small and globular). Severely damaged mitochondria were those showing loss of Δψ<sub>m</sub>. A total of 220 cells were counted for each concentration. For each mitochondrial shape class, data are expressed as percent cells compared with total cells counted (average ± SEM).

The effect of PYRs on nuclear morphology was evaluated using Hoechst-33258 assays according to Gonzalez et al. (2008), with minor modifications. This fluorochrome is a water-soluble compound that has been long used as a sensitive DNA-specific dye in characterizations of chromosomal condensation and fragmentation events. Hoechst-33258-related blue fluorescence appears enhanced after chromosomal condensation. This assay has been used in studies of chemical-induced disruption of nuclear integrity (Elstein and Zucker, 1994; Kim et al., 1988; Labarca and Paigen, 1980), including assessments of rat brain astroglia damage after exposure to anticholinesterase insecticides (Guizzetti et al., 2005). DNA labeling with Hoechst-33258 should not be used as an unequivocal proof of chemical-induced genotoxicity according to Organisation for Economic Co-operation and Development (OECD) regulations.

C6 cells (6 × 10<sup>4</sup> cells/well) were grown on glass cover slips in 12-well plates for 24 h. Then, cells were exposed for 24 h to individual PYRs (EC<sub>15/10</sub>, EC<sub>15</sub>, EC<sub>30</sub>, or EC<sub>max</sub>, as previously estimated in the MTT assays, see Table 1), or to the quaternary mixture described in Section Assessment of Cell Viability by the MTT Assay, as stock and following serial dilutions

**TABLE 1.** Estimation of Low-Effective Benchmark Concentrations for Cell Viability

Insecticide	Benchmark Concentration Levels (μM)		Coefficients of Goodness of Fit		NOEC (μM)	Relative Potency Factor (RPF)	EC <sub>15</sub> , DM-Equivalent Concentration (μM)
	EC <sub>15</sub>	EC <sub>30/max</sub>	R <sup>2</sup>	R <sup>2</sup> Adj.			
α-CYP	7.8 ± 1.1	30	0.94	0.90	1	0.64	5.00
DM (index)	5.0 ± 0.9	25	0.89	0.81	0.1	1	5.00
BF	16.1 ± 0.3	30.8 ± 1	0.99	0.98	5	0.31	5.00
TF	37.3 ± 2.3	50	0.87	0.75	5	0.13	5.00

EC<sub>15</sub>, EC<sub>30</sub>, and NOEC levels for cell viability assays were computed using mitochondrial metabolic activity as an endpoint (MTT test) in 24-h exposure assays. Although PYRs are poorly soluble in aqueous medium, there were a few assays for which EC<sub>30</sub> was estimated beyond the concentration range examined. In these cases, EC<sub>max</sub> levels (ie, the maximum concentration level examined) are informed instead of actual EC<sub>30</sub>s. R-squared (R<sup>2</sup>) statistical measures describing how close the data are to the fitted regression curves were high. In all cases, the goodness of fit was acceptable after computing adjusted R<sup>2</sup> coefficients (R<sup>2</sup> Adj.) to control for model overfitting. NOECs were estimated by 1-way ANOVA followed by Dunnett *post hoc* test. The RPFs were computed as the ratio of the EC<sub>15</sub> of the most potent PYR (DM, considered as the index chemical) and the EC<sub>15</sub> of each PYR. Thus, all compounds selected to construct the test mixture may be expressed in DM-equivalent concentrations.

0.05×, 0.1×, and 0.2×. Then, cells were washed twice with PBS and fixed with PFA-S in PBS for 20 min at RT. Finally, cells were washed with PBS and stained with 1.5 mg/ml Hoechst-33258 for 10 min. Cells were washed with PBS and mounted on glass microscope slides. Normal and anomalous nuclear figures were classified based on morphological landmarks described elsewhere (Alaimo *et al.*, 2011; Fenech *et al.*, 2011). A categorical system was used to typify and count nuclear shapes as follows: normal, swollen (ie,  $\geq 2.5$  times larger than normal nuclei), elongated (ie,  $\geq 2.5$  times nucleus enlargement in 1 direction), bilobulated, micronuclei, fragmented, and nuclear buds. A total of  $10^3$  cells were counted in each single-compound assay. Results are expressed as percentage of each shape category related to total cells counted (average  $\pm$  SEM). Samples were examined using a Nikon fluorescence microscope Eclipse E600 and TRITC filters ( $\lambda_{\text{ex}}$ : 528–553 nm;  $\lambda_{\text{em}}$ : 600–660 nm). The images were captured by a Nikon CoolPix5000 camera (Nikon Instech Co, Japan). Digital pictures were analyzed using ImageJ software.

**Data modeling.** Data were analyzed using SigmaPlot software, v.10.0 (Systat Software Inc, California). Logistic 3-parameter modeling was used to estimate benchmark levels in MTT assays.  $EC_{15}$  and  $EC_{30}$  values were computed as concentration levels producing 15% and 30% decline in the MTT assay reaction product compared with the corresponding vehicle-control cultures, respectively. When  $EC_{30}$  could not be estimated, the maximum concentration examined of the indicated PYR ( $EC_{\text{max}}$ ) was used as benchmark concentration. A default  $P$  value of .05 was used to test the goodness of fit.

**Analysis of acidic vesicle organelles by fluorescence microscopy.** The lysosomal compartment is the main site for degradation of a variety of macromolecules, including proteins, carbohydrates, nucleic acids, and lipids (Saftig, 2005). Fluorescence microscopy was used to study changes in the structure of acid vesicle organelles (AVOs) such as mergers or fissions. Briefly, C6 cells ( $6 \times 10^4$  cells/well) were grown on glass coverslips in 12-well plates, and exposed for 24 h to the quaternary mixture of PYRs described in Section Assessment of Cell Viability by the MTT Assay. Then, cells were washed with PBS and stained with 200 nM LysoTracker Red DND-99 (Molecular Probes, Invitrogen) for 30 min at 5%  $CO_2$  and 37°C, under darkness. Samples were washed and fixed as described in Section Cell Morphology. Nuclear labeling was performed using Hoechst-33258 dye and examined under a fluorescence microscope (Olympus IX-81, Olympus Corp, Japan) as indicated in Section Analysis of AVOs by Fluorescence Microscopy. The diameters of AVOs were measured from digital pictures by using ImageJ software. Fifty cells were examined at each concentration (1000 acidic vesicles per concentration). The area of individual AVOs was measured as described in Gorojod *et al.* (2015). The results are expressed as mean ( $\mu\text{m}$ )  $\pm$  SEM.

**Statistical analysis.** Statistical analyses were carried out by Student's  $t$  test and ANOVA followed by Student-Newman-Keuls *post hoc* test. No observable effect concentration (NOEC) was estimated by 1-way ANOVA followed by Dunnett *post hoc* test. Pearson's  $r$  correlation analyses were also carried out. A  $P < .05$  was set as the criteria for statistical significance. All analyses were conducted using GraphPad Prism 4 software (GraphPad Software, San Diego, California). Digital pictures were assembled using Adobe Photoshop (8.0.1).

## RESULTS

### PYRs Induce Cytotoxicity

C6 cell morphology and viability assessments were carried out to identify relevant exposure levels for the characterization of PYR-induced damage at particular markers of cellular physiology. In a preliminary study using the MTT assay, we found no significant effects of 0.1% DMSO vehicle on cell viability. Besides, the increase in FBS from 2% to 10% final concentration caused a mild growth-promoting effect (data not shown). Accordingly, the culture medium was alternatively supplemented with 2% and 10% FBS in independent assays to analyze the influence of serum on cell susceptibility. C6 cell viability was examined after 4- to 48-h exposure to PYRs.

The MTT assays showed a time- and concentration-dependent decrease in cell viability using 2% FBS (Figure 2). In general, C6 cells showed a marked decline in viability after 24-h exposure to PYRs. A decrease in mitochondrial dehydrogenase activity was evident after 12-h exposure to BF and TF ( $P < .0001$ ), and at a longer time (ie, 24 h) after exposure to DM and  $\alpha$ -CYP ( $P < .0001$ ) compared with control cells. In addition, there were similar trends of concentration-related decrease in response at 24 and 48 h for DM ( $F_{5,41} = 17.7$ ) and  $\alpha$ -CYP ( $F_{5,38} = 127.4$ ) (for the main effect of treatment,  $P < .0001$ ); instead, more marked reductions of viability were observed at 48 h than at earlier times for TF and BF ( $P < .0001$ ). Logistic fits with high regression factors confirmed trends for a concentration-dependent decrease in cell viability for all PYRs examined (Figure 2, right column), and allowed estimating benchmark levels marking low-ECs used in other single-compound and mixture assays in this work. At 24-h exposure assays,  $EC_{15}$  levels ranged from 5.0 to 37.3  $\mu\text{M}$  with  $\alpha$ -CYP and DM exhibiting the most potent cytotoxic action (Table 1). Thus, time-concentration-response assays indicated that approximately  $10^1$   $\mu\text{M}$  exposures were in all cases effective to produce alterations in viability. A 10% FBS supplement during incubation either attenuated or abolished the aforementioned effects (data not shown). Altogether, the MTT assays carried out after single-compound exposure to PYRs allowed selecting  $t_{24 \text{ h}}$  as an appropriate testing time to compare responses obtained using 2% FBS medium in additional cellular and biochemical studies.

PYRs produced concentration-related changes in NR accumulation, suggestive of a biphasic response of the lysosomal system (Figure 3). For all PYRs, the main effect of the treatment was statistically significant ( $P < .0001$ ):  $\alpha$ -CYP ( $F_{5,37} = 10.3$ ), DM ( $F_{5,39} = 7.4$ ), BF ( $F_{5,38} = 15.6$ ), and TF ( $F_{5,36} = 20.3$ ). NR retention was increased up to 30% over DMSO control after exposure to low levels of all PYRs, except for  $\alpha$ -CYP. Such an increase in lysosomal retention of NR may suggest an increase in the number and/or average size of lysosomal vesicles. Moreover, a decrease in NR retention was evident at higher PYRs concentrations. Poor solubility in aqueous solutions did not allow for examining DM concentrations above 25  $\mu\text{M}$ , restricting a confirmation of a biphasic trend for this compound.

Cell morphology was also altered after 24-h exposure to PYRs. Figure 3 shows DIC microscopy findings in DMSO and PYR-treated cultures (Figs. 3B, microphotographs a and b–e, respectively). After exposure to PYRs, C6 cells presented an apparent increase in cytoplasmic vacuolization (see b), refined and retracted cell soma processes (see c and d), membrane lamellipodia (see e), and a higher frequency of round-like shapes. Loss of adhesion to the culture dish substrate was also observed (see b–e). Moreover, reduced cell area became evident at the higher exposure levels examined: for

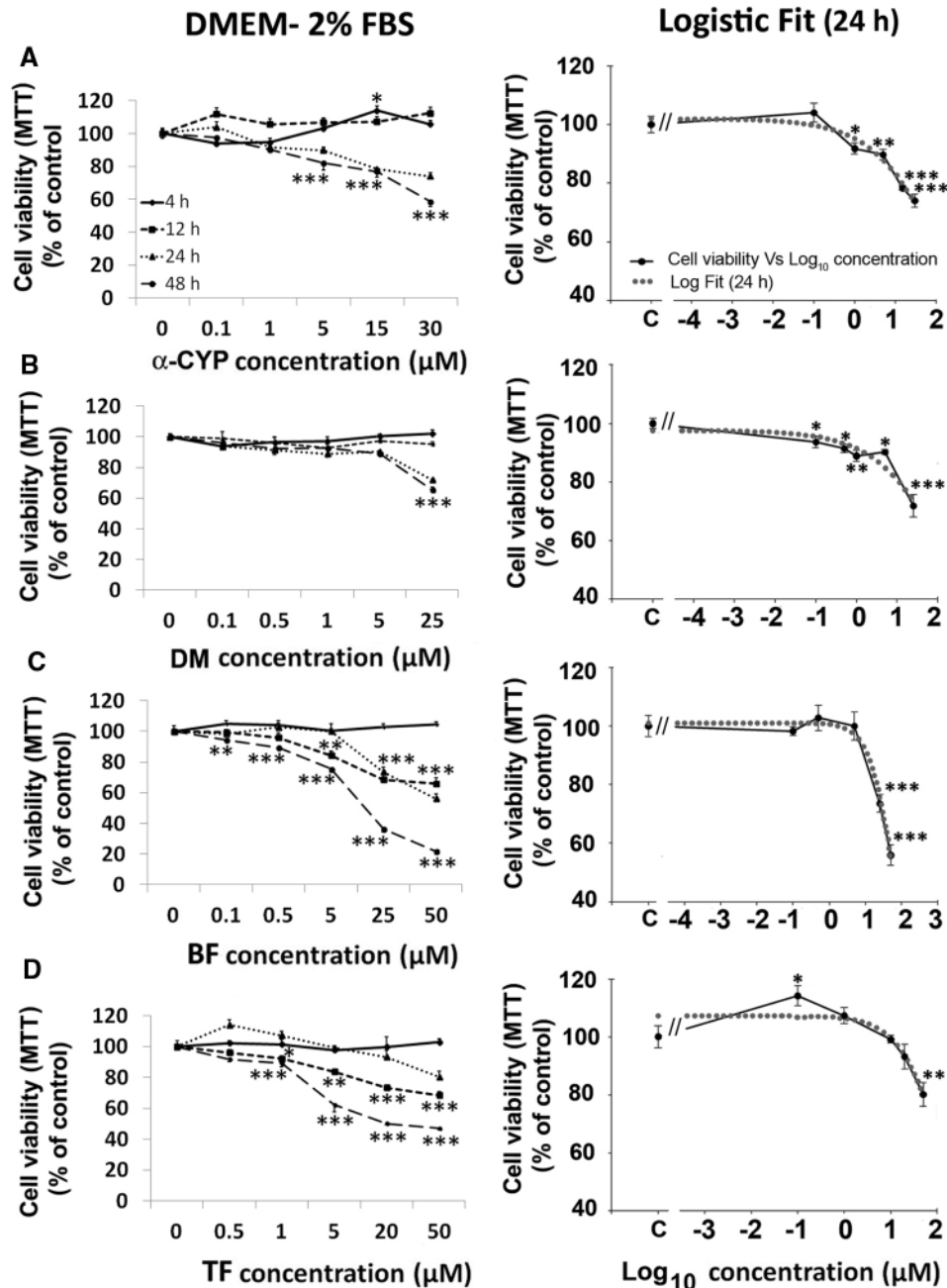


FIG. 2. PYRs induce time- and concentration-dependent cytotoxicity. C6 cells were exposed to increasing concentrations of A,  $\alpha$ -cypermethrin ( $\alpha$ -CYP); B, deltamethrin (DM); C, bifenthrin (BF); and D, tefluthrin (0.1–50  $\mu$ M) for 4–48 h in the presence of 2% fetal bovine serum (FBS), and viability was measured by the 3-(4,5-dimethyl-thiazol-2-yl)-2,5-diphenyl-tetrazolium bromide (MTT) assay. The results are expressed as percent control (mean  $\pm$  SEM). Concentration-effect data were fit using logistic models (panels on the right). For the sake of clarity, statistical significance asterisks for 24 h experiments were omitted in the cell viability curves on the left, and are indicated in the logistic fit curves at right (24 h). For PYR-treated cultures compared with dimethylsulfoxide (DMSO) control (C): \* $P < .05$ , \*\* $P < .01$ , \*\*\* $P < .001$ .

30  $\mu$ M  $\alpha$ -CYP and 50  $\mu$ M BF, 46%  $\pm$  3.3%, and 41%  $\pm$  2.8%, respectively (mean cell area decline  $\pm$  SEM;  $P < .001$ ).

#### Alterations in Nuclear Integrity

To explore whether PYRs may affect nuclear morphology, C6 cells were stained with the Hoechst-33258 dye and analyzed by fluorescence microscopy (Figure 4). In control cultures, C6 cells showed typical ellipsoid shapes, and anomalous nuclei were rarely observed (Figure 4A, a), in agreement with that described elsewhere (Alaimo et al., 2011; Guizzetti et al., 2005; Labarca and

Paigen, 1980; Wätjen et al., 2002). In general, a concentration-related decrease in normal-shape rates was observed after exposure to PYRs, with threshold levels for nuclear aberration apparent at low- $\mu$ M concentrations. The most frequent nuclear alterations found after 24-h exposure to PYRs were bilobulated and condensed nuclei (Figs. 4A, images e and f); nuclear buds and micronuclei were also observed (Figs. 4A, d and g). The extent of the decrease in normal-shape rates after exposure to an EC<sub>15</sub>/10 level (1:10 dilution of the EC<sub>15</sub> estimated based on MTT assay data) was as follows:  $\alpha$ -CYP: 25%  $\pm$  1.2% ( $F_{4,19} = 13.3$ ); DM:

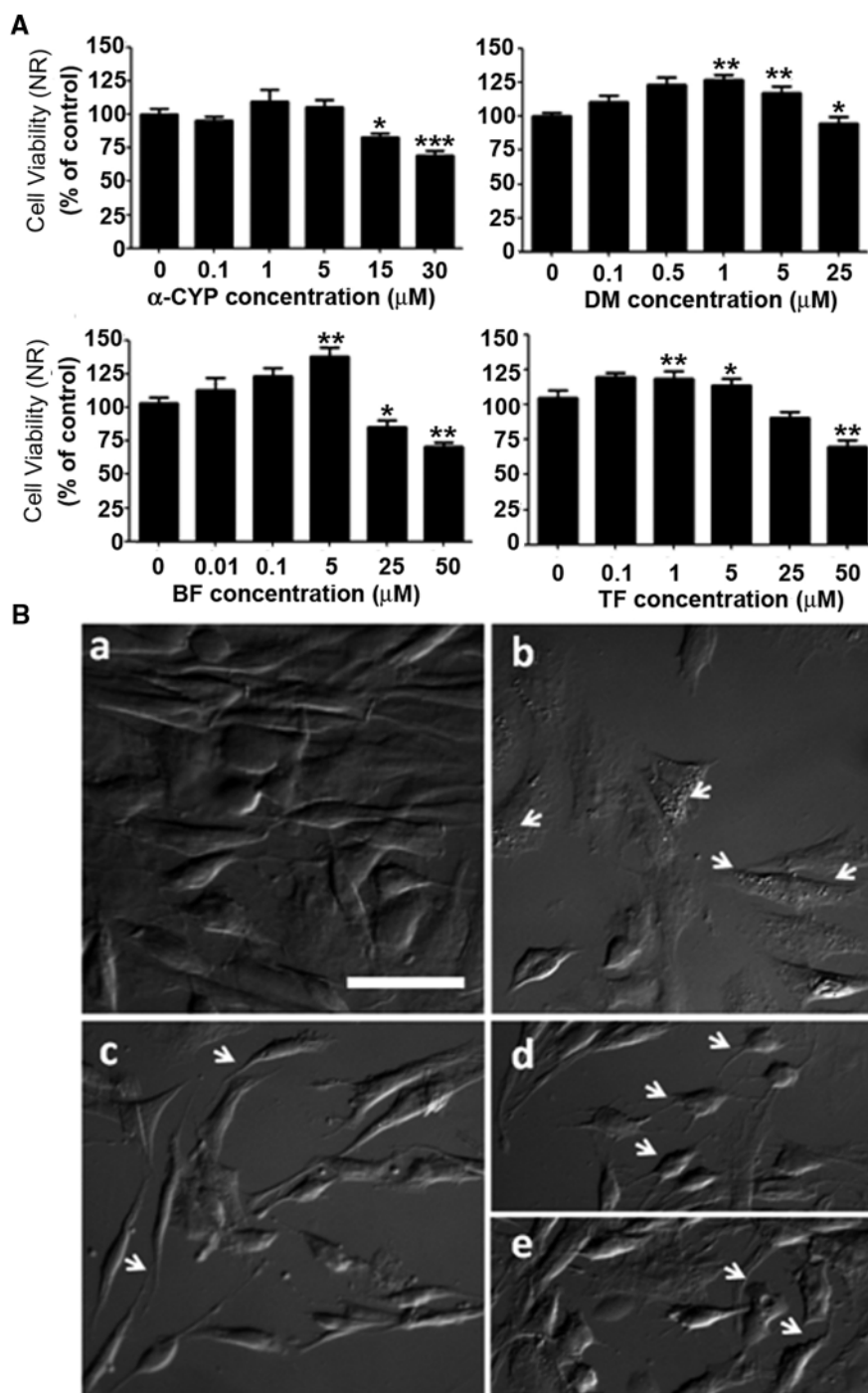


**FIG. 3.** PYRs cause alterations in lysosomal integrity and cell morphology. Panel A, Cell viability was further determined using neutral red accumulation assays after 24-h exposure to PYRs. In general, activation of the lysosomal system was evident at low- $\mu\text{M}$  levels, while a decline in response was observed at higher concentrations. Viability is expressed as % control, mean  $\pm$  SEM. For pairwise comparisons between DMSO- and PYR-treated cells: \* $P < .05$ , \*\* $P < .01$ , \*\*\* $P < .001$ . Panel B, differential interference contrast microscopy was used to evaluate morphological alterations in cell soma shape and processes. a, DMSO control; b, 30  $\mu\text{M}$   $\alpha$ -CYP; c, 50  $\mu\text{M}$  BF; d, 30  $\mu\text{M}$   $\alpha$ -CYP; and e, 25  $\mu\text{M}$  DM. Scale bar: 50  $\mu\text{m}$ .

26%  $\pm$  2.8% ( $F_{4,19} = 36.4$ ); BF: 38%  $\pm$  1.5% ( $F_{4,23} = 259.8$ ); and TF: 27%  $\pm$  1.2% ( $F_{4,24} = 83.2$ ) ( $P < .0001$ ).

#### Changes in Mitochondrial Integrity and $\Delta\psi_m$ Dissipation

We also investigated the potential association of the effects of PYRs on cell viability with changes in mitochondrial

morphology and  $\Delta\psi_m$  dissipation. To this end, we used MitoTracker Red assays. In DMSO-treated cultures, the mitochondrial network distributed throughout the cell soma and cellular processes, mostly exhibiting a tubular appearance, as expected from previous works (Alaimo et al., 2011, 2014; Pendergrass et al., 2004). After exposure to low- $\mu\text{M}$  PYR levels

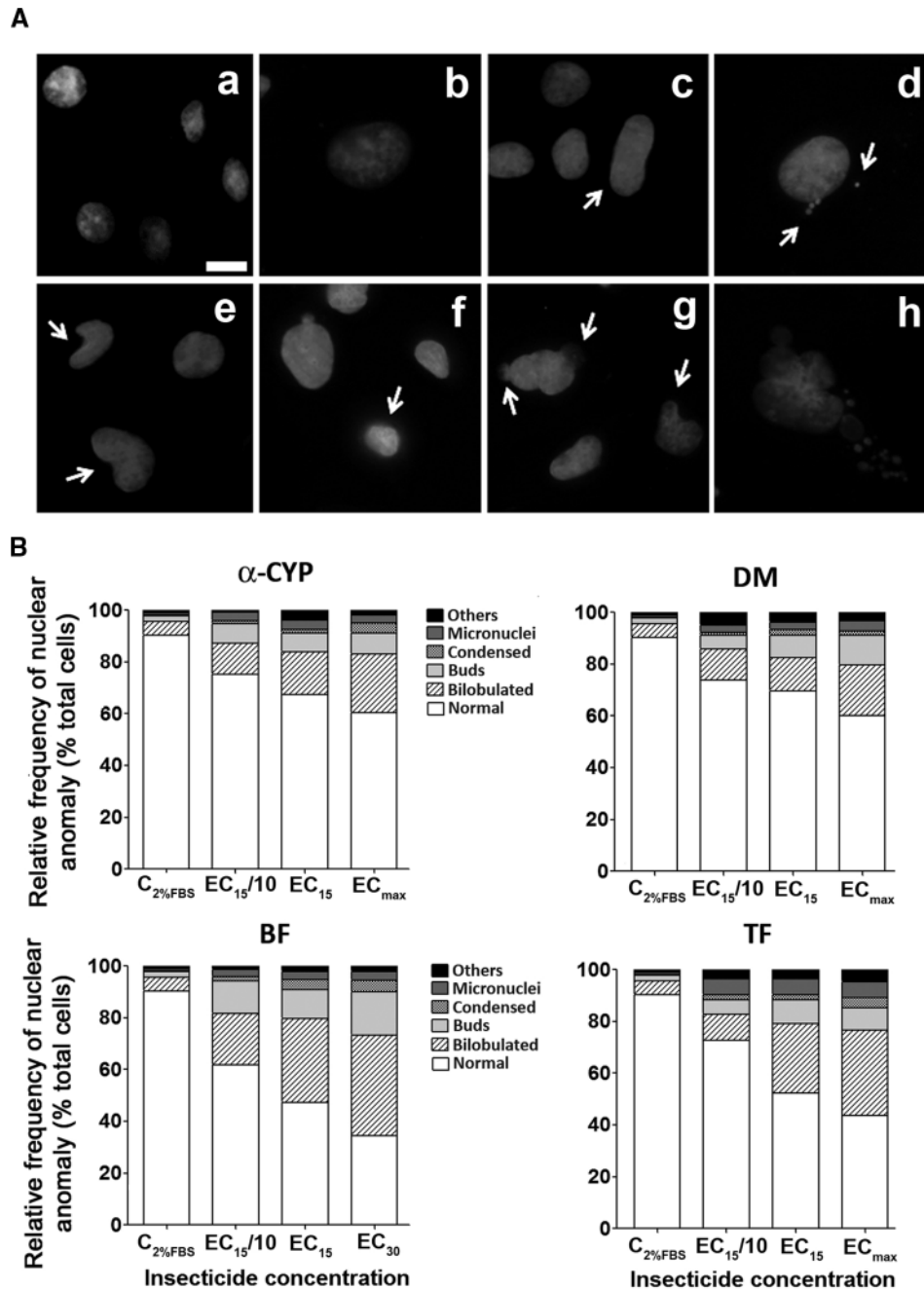


FIG. 4. PYRs cause alterations in nuclear integrity. After 24-h exposure to PYRs, C6 cells were fixed, stained with Hoechst-33258 and analyzed by fluorescence microscopy. Panel A, In general, Hoechst-33258 accumulation was restricted to the nuclear region, depicted by a round shape in DMSO-treated cultures, ie, indicative of the normal C6 cell nuclear shape (see a). Nuclear aberrations were classified as follows: swollen (b), enlarged (c), micronuclei (d), bilobulated (e), condensed (f), nuclei with buds (g), and fragmented (h). Panel B, Relative frequencies of nuclear shape anomalies are expressed as % total cells counted. Less frequent anomalies (< 4%), such as swollen, enlarged, and fragmented nuclei, were jointly classified as "others." Concentration-dependent increases in anomalous pyknotic shapes were evident at  $\geq$  effective concentration (EC)<sub>15</sub>/10 (ie, a benchmark concentration for cell viability). Total number of nuclei observed per concentration = 1000.

ineffective to cause evident changes in cell viability (see MTT assays in Figure 2), an imbalance in the fusion/fission equilibrium was evident (Figure 5). Furthermore, a decrease in the number of cells presenting tubular mitochondria was observed at low-exposure levels as follows:  $\alpha$ -CYP  $46\% \pm 8.7\%$  ( $F_{4,24}=264.3$ ), DM  $31.9\% \pm 4.5\%$  ( $F_{4,22}=781.6$ ), BF  $44.7\% \pm 3.3\%$  ( $F_{4,24}=652.8$ ), and TF  $24.4\% \pm 6.02\%$  ( $F_{4,24}=391.6$ ) ( $P < .0001$ ). This decrease was concomitant with an increase in the percentage of cells displaying intermediate mitochondria:  $\alpha$ -CYP  $48\% \pm 11.4\%$

( $F_{4,24}=32.08$ ), DM  $52.9\% \pm 8.6\%$  ( $F_{4,20}=40.1$ ), BF  $34\% \pm 3.6\%$  ( $F_{4,20}=46.07$ ), and TF  $61.5\% \pm 9.2\%$  ( $F_{4,19}=33.8$ ) ( $P < .0001$ ).

Moreover, the number of cells exhibiting  $\Delta\psi_m$  dissipation was higher at most of the concentrations examined. Fragmented mitochondria were detected in approximately 90% of total cells at the highest exposure levels. These results demonstrate that  $10^2$ – $10^4$  nM levels of PYRs may push the fusion/fission equilibrium toward mitochondrial fission, and that this effect is accompanied by  $\Delta\psi_m$  dissipation. Interestingly, when  $\geq$



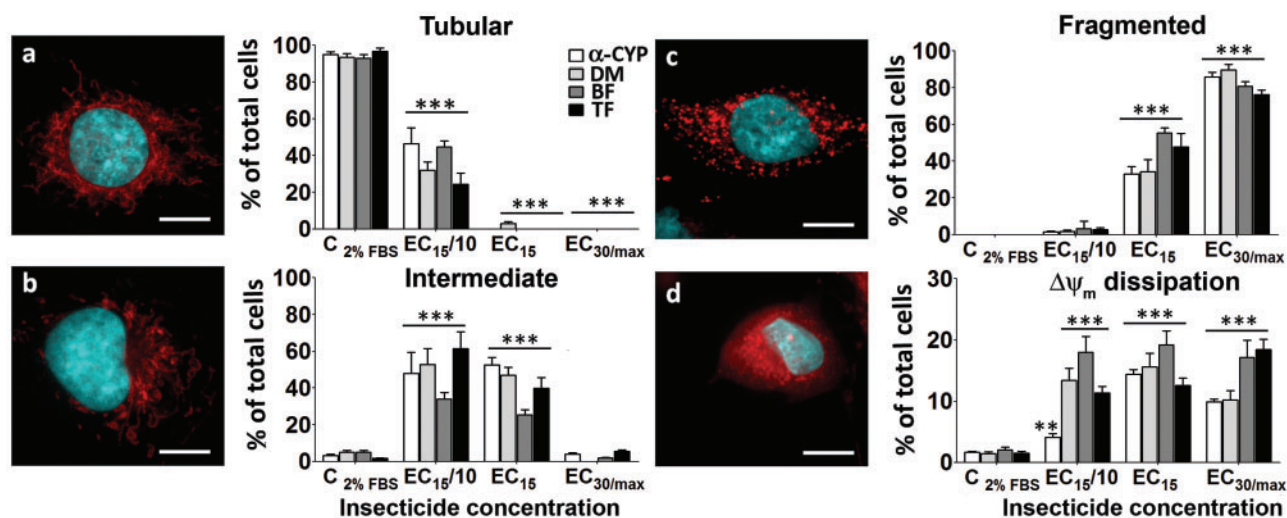


FIG. 5. Effects of PYRs on mitochondrial network integrity. PYRs caused alteration of the mitochondrial network and membrane potential. Left: photomicrographs show nuclear and mitochondrial labeling with Hoechst-33258 and MitoTracker Red CMXRos dyes, respectively, after 24-h exposure to PYRs. The mitochondrial network structure was classified using a categorical system as follows: A, tubular; B, intermediate; C, fragmented; and D, dissipation of membrane potential. The total number of cells observed per concentration was 220. Scale bar: 20  $\mu$ m. Right: frequencies of mitochondrial shapes are expressed as percent total cells of at least 3 experiments, mean  $\pm$  SEM. Note that fragmented mitochondria increase in parallel to a decrease in tubular morphology. \*\* $P < .01$ , \*\*\* $P < .001$ , for PYR-treated cultures compared with control (cells cultured in DMEM containing 2% FBS).

EC<sub>15</sub> levels for C6 cell viability (Figure 2) were used, the earlier mitochondrial findings cooccurred with increased rates of nuclear condensation (Figs. 4A, panels c and d and Figs. 8A and B, respectively). In fact, approximately 90%–95% of cells exhibited both  $\Delta\psi_m$  dissipation and chromatin condensation. Moreover, inverse correlations ( $r = -0.95$  to  $-0.99$ ) between mitochondrial fission (ie, % cells with fragmented mitochondria) and cell viability (MTT assay, % control) were computed for all PYRs, suggesting some relationship between the structural and functional aspects examined with these mitochondria-related assays.

#### A Mixture of Sub- $\mu$ M Levels of PYRs Causes a Decrease in C6 Cell Viability

We explored further whether the single-compound actions observed in C6 cells do cumulate as predicted by the dose-addition theory (Berembaum, 1985), under the assumption of a common primary MOA for PYRs (Soderlund et al., 2002).

**MTT assays.** We selected a mixture of low-effective levels of  $\alpha$ -CYP, DM, BF, and TF based on the information collected in the MTT assays (Figure 2), and relative potencies were estimated taking DM as an index chemical (DM<sub>IC</sub>) (Table 1). If the dose-addition theory assumptions ruled the joint effect of the quaternary mixture, the effect of a 1 $\times$  mixture solution consisting of equitoxic EC<sub>15</sub> levels of each compound would be expected to be statistically indistinguishable from that of from that of 20  $\mu$ M DM<sub>IC</sub>. Thus, we hypothesized an approximately 25% decrease in cell viability as a default prediction for the test mixture (see hypothesis construction scheme in Figure 6A). This mixture assay was not intended to be a rigorous assessment of cumulative effects but rather a preliminary approach to ascertain if any potential antagonism or synergism may occur with this exposure scheme.

Figure 6B shows the effects of the test mixture in MTT assays using 2% and 10% FBS. The mixture caused significant concentration-related changes in cell viability (for the main

effect of treatment,  $P < .01$ ). An average 36.5% decrease in viability was observed at the highest concentration compared with the DMSO control ( $P < .0001$ ) using 2% serum (Figure 6B). This decrease was 11.5% greater than the 25% expected *a priori* based on the DM<sub>IC</sub> equivalent concentrations of all PYRs combined in the stock mixture (compare theoretical vs empirical joint actions in Figs. 6A and B, respectively). The difference between C6 cells treated with a 0.2 $\times$  mixture dilution (comprising 1.6  $\mu$ M  $\alpha$ -CYP + 1.0  $\mu$ M DM + 3.2  $\mu$ M BF + 7.5  $\mu$ M TF) and vehicle-control cells was not statistically significant. Moreover, no changes in cell viability were observed after exposure to 1:10 and 1:20 mixture dilutions (Figure 6B). Last, 10% FBS completely abolished the decrease in viability induced by mixture 1 $\times$ , consistent with the apparently protective effect of serum observed in single-compound assays.

**Hoechst-33258 assays.** Figure 7A shows nuclear integrity after joint exposure to all PYRs. The mixture caused a concentration-dependent decrease in the number of normal nuclei compared with DMSO-control, as follows: 24.6%  $\pm$  6.8%, 35.1%  $\pm$  7.1%, and 46.4%  $\pm$  4.2% ( $F_{4,19} = 12.9$ ,  $P < .0001$ ), at 0.1 $\times$ , 0.2 $\times$ , and 1 $\times$  mixture levels, respectively, which was accompanied by increased rates of nuclear aberrations, even at the lowest concentrations examined (ie, 0.05–0.1 $\times$ ) (Figure 7A). Furthermore, a 0.05 $\times$  mixture level produced increased counts of micronuclei (2-fold,  $F_{4,16} = 5.3$ ,  $P < .01$ ), bilobulated (1.9-fold,  $F_{4,18} = 15.9$ ,  $P < .0001$ ), and condensed (28-fold,  $F_{4,16} = 14.4$ ,  $P < .0001$ ) nuclei, and there was a 7.5-fold increase in nuclei with buds ( $F_{4,16} = 14.2$ ,  $P < .001$ ).

**MitoTracker Red assay.** As observed with single compounds, the mixture caused changes in the mitochondrial network structure and induced  $\Delta\psi_m$  dissipation (Figure 7B). Increased rates of mitochondrial fission were evident. Furthermore, a decrease in the number of cells carrying preserved tubular network was observed at all test concentrations; even the lowest mixture level examined, 0.05 $\times$ , caused a decrease of 50%  $\pm$  1.5% ( $F_{4,15} = 829.1$ ,  $P < .0001$ ). The presence of intermediate mitochondria

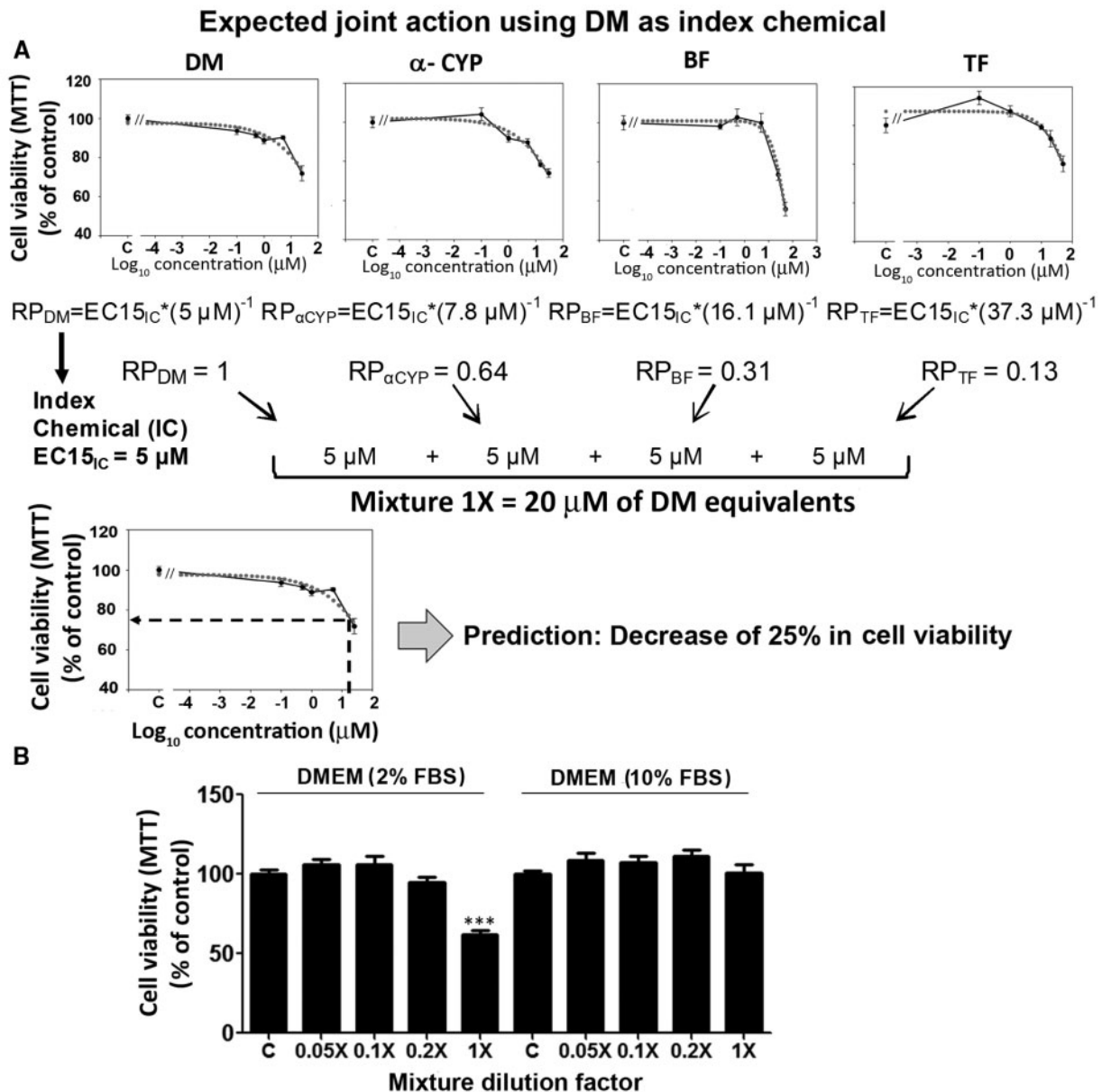


FIG. 6. C6 cell viability after a low-level exposure to a mixture of PYRs. Panel A shows a schematic synthesis of the default hypothesis selection and testing process. Single-compound  $EC_{15}$  levels were estimated using MTT assay data (Figure 2 and Table 1). According to the default assumption and selecting DM as index chemical the stock mixture was expected to produce a 25% decrease in cell viability. Panel B shows the results of the MTT assays conducted after 24-h exposure to the PYR mixture. A decrease in cell viability at the highest mixture concentration was observed using 2% FBS (left chart). A 10% FBS supplement had a protective effect against PYR action. Viability is expressed as percent control, mean  $\pm$  SEM. For comparisons between PYR-treated and vehicle-exposed cultures (DMEM 2% FBS): \* $P < .05$ , \*\*\* $P < .001$ .

was by far the most frequent morphological observation with 12-fold higher rate than in vehicle-exposed cells at 0.05–0.2 $\times$  mixture levels ( $F_{4,16} = 14.6$ ,  $P < .0001$ ). This increase was not evident after exposure to the undiluted mixture (1 $\times$ ) which produced a high rate of fragmentation (175-fold compared with control;  $F_{4,12} = 254$ ,  $P < .0001$ ). Furthermore, an increased number of cells with  $\Delta\psi_m$  dissipation was observed at all mixture concentrations, reaching a peak at a 0.2 $\times$  level (ie, 12-fold increase;  $F_{4,13} = 27.2$ ,  $P < .0001$ ). Thus, the mixture caused a marked perturbation in the fusion/fission equilibrium of the mitochondrial network dynamics, extending the findings shown in Figs. 2 and 5.

LysoTracker Red DND-99 assays. Last, we conducted LysoTracker Red DND-99 assays to evaluate the responsiveness of the acidic compartment after 24-h exposure to the mixture. Bright field microscopy suggested that PYRs-treated cells presented refringent vesicle-like shapes in the cytoplasm; this observation was not evident in DMSO-exposed cells (Figure 8A). We observed an increased rate of large-size AVOs and a reduction in their total count per cell after exposure to the mixture. In general, these changes were related to mixture concentration. The average vesicle diameter was: control,  $0.49 \pm 0.0002 \mu m$ ; mixture (mix) 0.1 $\times$ :  $0.78 \pm 0.0003 \mu m$ ; mix 1 $\times$ :  $0.93 \pm 0.0030 \mu m$ ; and  $P < .0001$ .

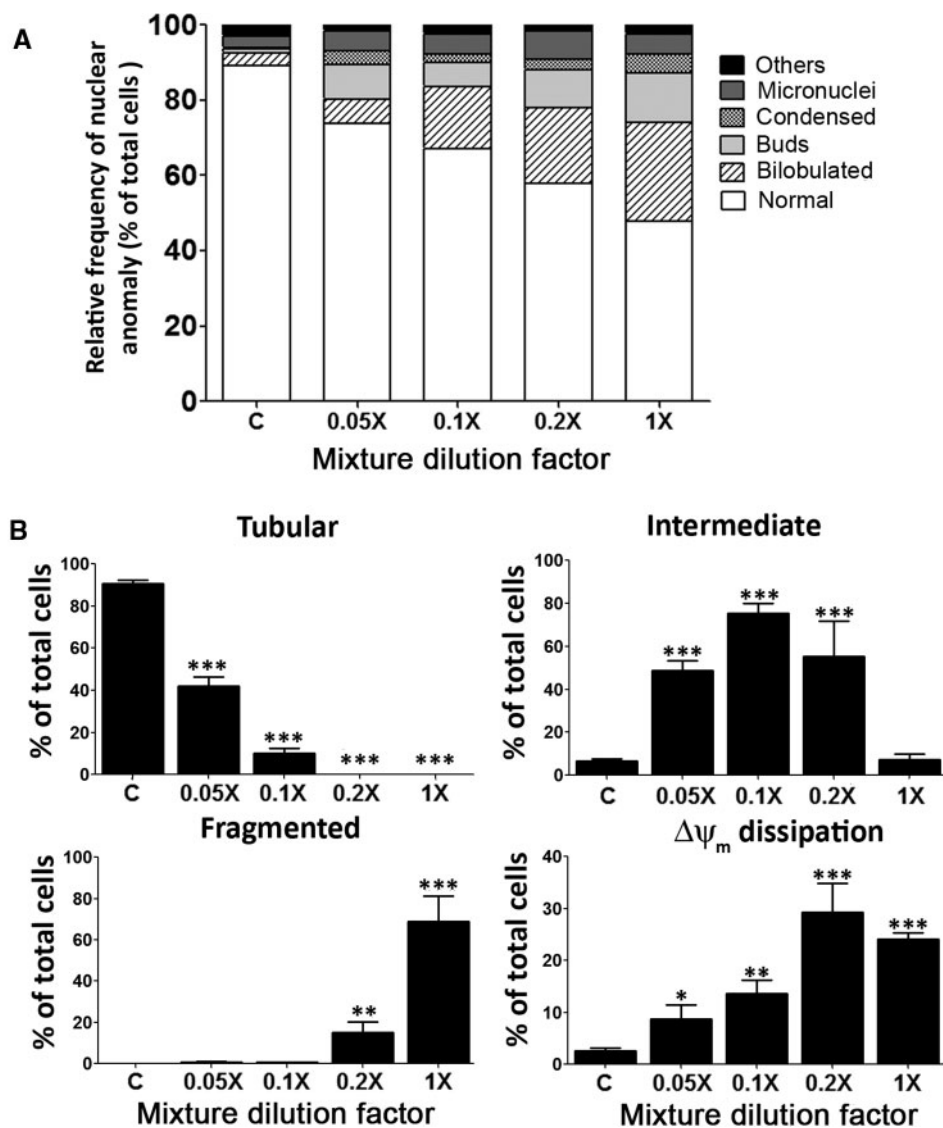


FIG. 7. Joint action of the PYR mixture on nuclear and mitochondrial integrity. Panel A, Evaluation of nuclear morphology using Hoechst-33258 assays after 24-h exposure to the mixture. Panel B, Concentration-response relationships for mitochondrial integrity using MitoTracker Red CMXRos. See classification of mitochondrial network shapes in Figure 5 legend. Results are expressed as relative frequency of nuclear anomaly (% of total cells counted, mean  $\pm$  SEM), from at least three independent experiments. For each mixture concentration, the total number of nuclei observed was 1000 for Hoechst-33258 assays, and 220 cells were examined for mitochondrial integrity assays. Statistical significance of differences between PYR-treated and DMSO control cultures (2% FBS): \* $P < .05$ , \*\* $P < .01$ , \*\*\* $P < .001$ .

## DISCUSSION

In this work, we showed that exposure to PYRs for 24 h impairs C6 cell viability. Considering single-compound and mixture assays, threshold levels for PYR-induced alterations in morphological and functional integrity spanned the  $10^1$ – $10^4$  nM range. Our results suggest that neuroglia-derived cells may be susceptible to physiological disruption after exposure to environmentally relevant levels of PYRs.

We found concentration-dependent adverse effects on the mitochondrial network architecture and function after single- (Figs. 2 and 5) and multiple- (Figs. 6 and 7) PYR exposure at  $10^{-2}$ – $10^1$   $\mu$ M concentrations. PYRs decreased mitochondrial dehydrogenase activity, increased  $\Delta\psi_m$  dissipation, and perturbed the fusion/fission equilibrium, ie, pushed the equilibrium toward mitochondrial fission. Noteworthy, a loss of typical tubular appearance in the mitochondrial network was

even observed after simultaneous exposure to individual concentrations well below single-compound threshold levels for cell viability (compare Figs. 5 and 7 with Figs. 2 and 3). Moreover, for all PYRs tested, concentration-related changes in the number of viable cells at 24 h correlated with the disruptive effect on the fusion/fission equilibrium. In addition, time-concentration-response experiments (MTT assay) showed an earlier onset of effects (ie, at 12 h) with a significant decrease in cell viability after exposure to BF and TF concentrations  $\geq 25$   $\mu$ M (Figure 2; compare with DM and  $\alpha$ -CYP). In general, in rats, lethality occurs within 12 h after acute oral exposure to lethal doses of PYRs (Wolansky and Harrill, 2008), and BF and TF have lower threshold doses for lethality than DM, CYP, and  $\alpha$ -CYP (WHO, 2010; Wolansky et al., 2006, 2007). Yet, the numerous differences between the *in vitro* conditions of our study and *in vivo* assessments after

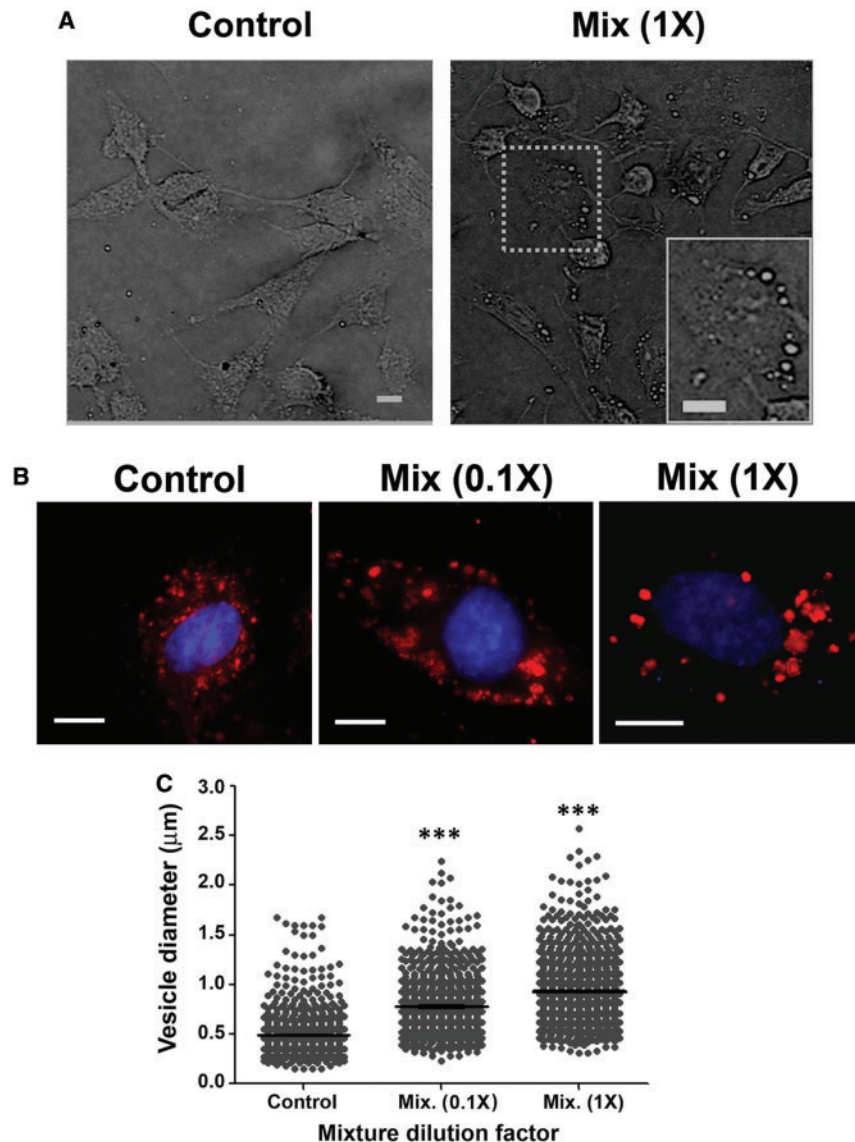


**FIG. 8.** Cumulative action of the PYR mixture on acidic vesicle organelles (AVOs). Bright field microscopy and LysoTracker Red DND-99 staining were carried out after 24-h exposure to 0.1 and 1 $\times$  mixture levels to evaluate PYR joint effects on AVOs. Panel A, Bright field microscopy analyses show alterations in the number of AVOs (see dotted line boxes in the microphotography). Panel B, C6 cells stained with LysoTracker Red DND-99 and costained with Hoechst-33258. All images represent merged fluorescent pictures. Panel C, Analysis of acidic vesicle diameters. Results are expressed in  $\mu\text{m}$ , mean  $\pm$  SEM. Statistical significance of differences between PYR-treated and DMSO-treated cultures (2% FBS): \*\*\* $P < .001$ . Scale bars = 10  $\mu\text{m}$ .

exposure to PYRs may hinder any comparison of viability impairment over time in C6 cells and lethality in laboratory animals.

Mitochondria are very plastic organelles, endowed with the ability to split as dispersed individual blocks or to arrange in complex interconnected networks displaying rapid shape interconversion (Bereiter-Hahn and Vöth, 1994; Sheridan and Martin, 2010). During mitosis as well as during apoptosis, the mitochondrial network is fragmented, resulting in a larger number of smaller mitochondria. In apoptosis, this phenomenon usually occurs before activation of caspases and the release of cytochrome c into the cytosol (Martinou and Youle, 2006). This enhanced fragmentation suggests a mechanistic link between changes in the mitochondrial network architecture and apoptosis. Consistent with this suggestion, we also observed alteration of  $\Delta\psi_m$  dissipation (Figure 5), which has been proposed to be a key event in the intrinsic

signaling pathway leading to apoptotic cell death after intracellular exposure to chemical stressors (Galluzzi et al., 2012). Braguini et al. (2004) examined the molecular actions of DM in mitochondrial fractions prepared from rat liver. Nanomolar levels of DM caused mitochondrial alterations in critical aspects of the organization of the membrane lipids, lipid-protein interactions relevant to oxidative phosphorylation, membrane permeability (ie, its  $\Delta\psi_m$  potential), and mitochondrial volume. Furthermore, several studies have demonstrated the ability of PYRs to increase reactive oxygen species (ROS), and progressive oxidative stress following increased rates of ROS generation has been proposed to lead to cell death (Gupta et al., 2013; Liu et al., 2009; Romero et al., 2012, 2015; Srivastava et al., 2012). In turn, increased intracellular levels of ROS may induce the opening of the mitochondrial permeability transition pore (Mattson and Kroemer, 2003). A ROS-induced cell death pathway involving mitochondrial fission and  $\Delta\psi_m$

dissipation has been proposed in C6 cells and cerebral astrocytes after exposure to manganese (Alaimo *et al.*, 2011; Gonzalez *et al.*, 2008). Studies of Maurya *et al.* (2012, 2016) reported overproduction of ROS, mitochondrial disruption, and cell death in cortical and hippocampal astrocytes after a 2-week daily oral exposure to CYP in weanling rats. Other *in vivo* studies in small rodents and *in vitro* studies in human cells are consistent with the occurrence of cytotoxicity in nervous system cells after exposure to PYRs, leading to astrogliosis, neuroinflammation, and apoptotic cell death in astroglia (Mense *et al.*, 2006; Singh *et al.*, 2011). However, most of these previous studies used exposure schemes with limited comparability (if any) to environmentally relevant scenarios of human exposure to PYRs.

In this study, low levels of PYRs were also effective to disturb the lysosomal compartment of C6 cells (Figs. 3A and 8). Lysosome vesicles make up a natural defense system engulfing and digesting potential chemical stressors. In our work, all PYRs except  $\alpha$ -CYP induced a biphasic response of lysosomes (Figure 3A): an increase in NR retention at  $10^0$ – $10^1$   $\mu$ M concentrations and a decrease at higher concentrations. LysoTracker Red DND-99 assays further demonstrated that PYRs induced an increase in the size of AVOs in parallel to a decrease in the number of these vesicles (Figure 8B). Concentration-dependent increases in the amount and/or size of lysosome vesicles at low-level exposures may be interpreted as gradual stages of activation evolving to counteract the damaging actions of PYRs. Lysosomal activation has been proposed to contribute to cell death in astroglia after exposure to neurotoxic metals (Gorojod *et al.*, 2015). In addition, a decrease in NR retention at above  $10^1$   $\mu$ M may indicate exhaustion of lysosomal capacity under extreme cytosolic levels of PYRs (Saftig, 2005).

In addition, increased rates of nuclear anomalies were evident after 24-h exposure to PYRs, even at concentrations below the threshold level for cell viability (Figs. 4 and 7A). The most frequent alterations were bilobulated and condensed nuclei, followed by micronuclei and buds, all of which are fairly consistent with descriptions of DNA instability and DNA damage-related apoptotic cell death (Bolognesi *et al.* 2011; Fenech, 2002; Fenech *et al.*, 2011). Our results are consistent with several studies in cultured cells (Çelik *et al.*, 2005; Liu *et al.*, 2009; Patel *et al.*, 2006), mouse bone marrow (Bhunya and Pati, 1990), and fish erythrocytes (Simoniello *et al.*, 2009), reporting greater rates of micronuclei, DNA fragmentation, and chromosome aberrations after exposure to several cyano- and noncyano-PYRs. Interestingly, most of these previous studies used much higher PYR concentrations, marking the sensitivity of C6 cells to the cytotoxic actions of PYRs. The molecular mechanism linking PYR exposure to DNA damage is presently unclear. The nuclear envelope microstructure has been proposed as a target site in ticks exposed to the PYR permethrin (Roma *et al.*, 2013). Thus, our results call for a comprehensive battery of assays to characterize nuclear integrity in nervous system cells *in vitro* and *in vivo* after low-level exposure to PYRs, such as an immunohistochemical assessment of nuclear envelope microstructure, and micronuclei and comet tests.

The findings of this work raise a concern about the poorly explored PYR actions targeting physiological aspects other than the neuronal system of VGSCs long proposed as the primary target site for all PYRs regardless of their type (Narahashi, 2000; Soderlund *et al.*, 2002). Types I and II PYRs cause distinctive neurobehavioral syndromes *in vivo* in adult rats, and this divergence is the most evident at high-effective oral doses (Weiner *et al.*, 2009; Wolansky and Harrill, 2008). Extensive *in vitro* studies using *Xenopus* oocytes, rat brain synaptosomes, a

neuroblastoma cell line, and a battery of electrophysiological and neurochemical endpoints are consistent with the canonical triple classification, ie, types I, II, and mixed I/II (Breckenridge *et al.*, 2009). Yet, the mechanistic divergence causing the proposed common-mechanism types would be hardly accounted by PYRs solely acting on the neuronal VGSC system (Aschner, 2000). In the context of characterizing PYR actions in nervous system cells, C6 cells have the advantage of having many morphological, functional, pharmacological, and toxicological features of astrocytes (Benda *et al.*, 1968; Cookson *et al.*, 1995; Posada-Duque *et al.*, 2015) but own a poor (if any) expression of VGSCs (Munson *et al.*, 1979; Sontheimer, 1994; Wang *et al.*, 1992). Furthermore, Hales and Tyndale (1994) reported that C6 cells do not present a functional GABA<sub>A</sub> receptor-mediated signaling, which hinders any attempt for a comparison of our work with the action of GABAergic drugs on PYR effects in rat brain synaptosomes published by Crofton and Reiter (1987). Neuronal voltage-gated calcium channels are also proposed to be relevant as alternative target sites accounting for type-I/type-II divergence in neurological effects (Shafer and Meyer, 2004; Soderlund *et al.*, 2002). In primary cultures of mouse cortical neurons,  $10^1$ – $10^2$  nM BF (ie, a concentration range found to be suprathreshold in our work), has been shown to be effective to alter synchronous calcium oscillations (relevant for cell morphology phenotype) with independence of actions on VGSCs, and apparent participation of signaling mediated by glutamate NMDAR receptors (Cao *et al.*, 2014). Although the EACC1 subtype of glutamate transporter is endogenously expressed and functional in C6 cells (Sims *et al.*, 2000), it remains to be established if glutamate-related pathways played a determinant role in our work. In addition, C6 cells present a remarkable mitochondrial sensitivity to peripheral benzodiazepine (PBD) receptor ligands: exposure to nM levels of PBD-like ligands causes a sequence of proapoptotic events similar to that observed in our work with all PYRs, including morphological restructuring of the mitochondrial network, increase in mitochondrial membrane potential dissipation, and apoptotic-like cell death (Chelli *et al.*, 2004; Shiraiishi *et al.*, 1991). Whatever the mechanism by which PYRs caused severe damage to C6 cell viability and nuclear integrity in a concentration-related manner, this mechanism would hardly involve the voltage-gated ion channels and receptor systems of neurons classically postulated as target sites for common and type-specific actions of PYRs in the nervous system.

In the light of the sensitivity of C6 cells in single-compound assays, ie, demonstrating harmful actions at low- $\mu$ M levels, we then explored the cumulative action of nM levels of multiple PYRs. PYRs have been proposed to have a similar primary MOA in neurons (Soderlund *et al.*, 2002). All the preparations of PYRs examined, except DM, were not classified using the type-I/type-II and T/CS canonical systems proposed approximately 35 years ago (Soderlund *et al.*, 2002). In addition, those classical studies of PYRs in laboratory animals were conducted using intravascular and intracerebroventricular routes, ie, not the oral gavage intubation that carries more relevance for humans. The studies using oral dosing and young adult rats indicate that DM causes a type-II, CS-like syndrome, and that BF causes a type-I, tremorigenic syndrome (Crofton and Reiter, 1984; Wolansky *et al.*, 2007). More recently, Weiner *et al.* (2009) conducted a comprehensive functional observational battery study that further supports a type-I like classification of BF and TF and a type-II classification of DM.  $\alpha$ -CYP has never been classified using a battery of neurobehavioral measures after oral exposure in rats, although all studies of racemate preparations of CYP consistently indicate that this compound produces typical type-II, CS-syndrome signs

of toxicity (Weiner et al., 2009; Wolansky and Harrill, 2008). Thus, the 4 compounds examined in our work represent the toxicological heterogeneity of PYRs to a great extent (Wolansky and Harrill, 2008). At the time of designing our study, a few reports had suggested dose addition as a plausible hypothesis for the joint actions of PYRs in nervous system cells. Cao et al. (2011) reported dose-additive actions of PYRs on VGSC inward sodium influx in primary cultures of cerebrocortical neurons. In addition, 2 *in vivo* studies in adult rats using low-level acute oral exposures and neurotoxicity as an endpoint strongly suggest that PYRs act jointly as predicted by the dose-addition theory (Marshall et al., 2013; Wolansky et al., 2009; Wolansky et al., unpublished data). In the present work, the stock mixture caused potential nonadditive effects on cell viability, and 0.05–0.2× mixture dilutions (ie, mostly consisting of  $10^{-1}$ – $10^1$   $\mu$ M levels shown to be subeffective in single-compound assays) were likewise subthreshold in MTT assays (Figure 6B). Yet, confirmation or rejection of additivity will require a selection of test mixture levels, mathematical modeling, and statistical testing protocols specifically designed to test cumulative actions under a similar *in vitro* coexposure scenario. Thus, we are not able to statistically compare the expected and experimental results obtained with the stock mixture in MTT assays (Figs. 6A and B, respectively). If the empirical 36.5% decrease in cell viability were not statistically different from the theoretically estimated 25%, then the MTT assay results would be potentially consistent with the additive effects of a mixture of PYRs recently reported by Romero et al. (2015) using different cell culture systems and oxidative stress assays, and by Johnstone et al. (2016) using a primary cortical network of neurons and glia as an *in vitro* experimental system, and spontaneous mean network firing rate as an endpoint. Noteworthy, when the same mixture level scheme (0.05–1× range) was examined using Hoechst-33258, MitoTracker Red CMXRos, and LysoTracker DND99 fluorescent dyes informing on nuclear integrity, mitochondrial network structure, and lysosomal status, threshold concentrations for C6 cell damage were observed at 10- to 100-fold lower levels than in MTT assays. It remains to be elucidated which mechanisms are operative to cause the earlier mentioned patterns of joint effects.

Our work and previous studies warn on the progressive damaging actions that PYRs may exert on nervous system cells at exposure levels below those producing evident clinical signs of acute toxicity. Astrocytes contribute to establishing structural bridges and signaling pathways in the nervous system, being able to modulate short- and long-term physiological and pharmacological responses in neurons, and to generate cytosolic calcium waves after neurotransmitter-mediated synaptic activity (Eroglu et al., 2008; Navarrete and Araque, 2014; Sofroniew and Vinters, 2010). More recently, it has been shown that astrocytes participate in learning and memory processes (Lee et al., 2014). Threshold PYR exposures for disruption of neuronal excitability in rat dorsal root ganglion neurons extend over an approximately  $10^{-1}$   $\mu$ M range (Tabarean and Narahashi, 1998). Furthermore, several studies have reported cardiovascular, endocrine, and developmental alterations after exposure to 0.1–50  $\mu$ M PYR levels (DeMicco et al., 2010; Du et al., 2010; Go et al., 1999; Kojima et al., 1988; Nishimoto et al., 1987; Pine et al., 2008; Spencer et al., 2001). The fact that low-nM concentrations of PYRs in the test mixture were disruptive of various critical indicators of C6 cell survival warns of the potential harmful effects of low-dose exposures to PYRs. This study using a cell line with an astrocytic lineage calls for future research efforts to determine to what extent the low-dose levels of PYRs may

exacerbate chronic nervous system disorders caused or influenced by aberrant neuron-glia interactions.

In conclusion, we found that single- or multiple-compound *in vitro* exposure of C6 cells to  $\geq 10^1$  nM levels of modern PYRs may cause adverse alterations in several homeostatic systems of cell physiology, promoting activation of signaling landmarks of apoptotic cell death. We describe these low-dose effects in astrocyte-like cells. Importantly, pharmacological and toxicological actions of PYRs in neuroglia have been mostly investigated at concentrations irrelevant to the health risks of these insecticides in humans. Thus, our work adds novel evidence on the vulnerability of the nervous system to sub- $\mu$ M levels of PYRs.

## ACKNOWLEDGMENTS

M.J.W. wants to express his gratitude to W. Kobel, S. Allen, C. Breckenridge, T. Pastoor, and F. Suarez, from Syngenta Crop Protection Inc, for a donation of scientific equipment used in this study.

## FUNDING

This work was funded by grant PICT-2007-1340, National Agency for Promotion of Science and Technology (ANPCyT), and PIP 0356, CONICET. Argentina Ministry of Science and Technology. M.J.W. is an Argentina National Research Council (ARG NRC) scientist and University of Buenos Aires (UBA) professor. M.L.K. is an ARG NRC scientist. The ARG NRC through its office of doctoral programs funded the research fellow positions of D.M.R. and B.G.B. at UBA School of Science, Department of Biological Chemistry.

## REFERENCES

- Abdel-Rahman, A., Shetty, A. K., and Abou-Donia, M. B. (2001). Subchronic dermal application of N,N-diethyl m-toluamide (DEET) and permethrin to adult rats, alone or in combination, causes diffuse neuronal cell death and cytoskeletal abnormalities in the cerebral cortex and the hippocampus, and Purkinje neuron loss in the cerebellum. *Exp. Neurol.* **172**, 153–171.
- Alaimo, A., Gorjod, R. M., Beauquis, J., Muñoz, M. J., Saravia, F., and Kotler, M. L. (2014). Deregulation of mitochondria-shaping proteins Opa-1 and Drp-1 in manganese-induced apoptosis. *PLoS One* **9**, e91848.
- Alaimo, A., Gorjod, R. M., and Kotler, M. L. (2011). The extrinsic and intrinsic apoptotic pathways are involved in manganese toxicity in rat astrocytoma C6 cells. *Neurochem. Int.* **59**, 297–308.
- Aschner, M. (2000). Interactions between pesticides and glia: An unexplored experimental field. *Neurotoxicology* **21**, 175–180.
- Benda, P., Lightbody, J., Sato, G., Levine, L., and Sweet, W. (1968). Differentiated rat glial strain in tissue culture. *Science* **161**, 370–371.
- Bereiter-Hahn, J., and Vöth, M. (1994). Dynamics of mitochondria in living cells: Shape changes, dislocations, fusion, and fission of mitochondria. *Microsc. Res. Tech.* **27**, 198–219.
- Berembaum, M.C. (1985). The expected effect of a combination of agents: the general solution. *J. Theor. Biol.* **114**(3), 413–431.
- Bhunya, S. P., and Pati, P. C. (1990). Effect of deltamethrin, a synthetic pyrethroid, on the induction of chromosome

- aberrations, micronuclei and sperm abnormalities in mice. *Mutagenesis* 5, 229–232.
- Bolognesi, C., Creus, A., Ostrosky-Wegman, P., and Marcos, R. (2011). Micronuclei and pesticide exposure. *Mutagenesis* 26, 19–26.
- Braguini, W. L., Cadena, S. M., Carnieri, E. G., Rocha, M. E., and de Oliveira, M. B. (2004). Effects of deltamethrin on functions of rat liver mitochondria and on native and synthetic model membranes. *Toxicol. Lett.* 152, 191–202.
- Breckenridge, C. B., Holden, L., Sturgess, N., Weiner, M., Sheets, L., Sargent, D., Soderlund, D.M., Choi, J.S., Symington, S., Clark, J.M., et al. (2009). Evidence for a separate mechanism of toxicity for the type I and the type II pyrethroids insecticides. *Neurotoxicology* 230(Suppl.1), S17–31.
- Cao, Z., Cui, Y., Nguyen, H. M., Jenkins, D. P., Wulff, H., and Pessah, I. N. (2014). Nanomolar bifenthrin alters synchronous Ca<sup>2+</sup> oscillations and cortical neuron development independent of sodium channel activity. *Mol. Pharmacol.* 85, 630–639.
- Cao, Z., Shafer, T. J., Crofton, K. M., Gennings, C., and Murray, T. (2011). Additivity of pyrethroid actions on sodium influx in cerebro cortical neurons in primary culture. *Environ. Health Persp.* 119, 1239–1246.
- Carpy, S. A., Kobel, W., and Doe, J. (2000). Health risk of low-dose pesticides mixtures: A review of the 1985-1998 literature on combination toxicology and health risk assessment. *J. Toxicol. Environ. Health B Crit. Rev.* 3, 1–25.
- Çelik, A., Mazmanci, B., Camlica, Y., Askin, A., and Cömelekoglu, U. (2005). Induction of micronuclei by lambda-cyhalothrin in Wistar rat bone marrow and gut epithelial cells. *Mutagenesis* 20, 125–129.
- Center for Disease Control and Prevention (CDC). (2015). Fourth National Report on Human Exposure to Environmental Chemicals. US Department of Health and Human Services. Available at: [http://www.cdc.gov/biomonitoring/pdf/fourth\\_report\\_updatedtables\\_feb2015.pdf](http://www.cdc.gov/biomonitoring/pdf/fourth_report_updatedtables_feb2015.pdf).
- Chelli, B., Lena, A., Vanacore, R., Da Pozzo, E., Costa, B., Rossi, L., et al. (2004). Peripheral benzodiazepine receptor ligands: Mitochondrial transmembrane potential depolarization and apoptosis induction in rat C6 glioma cells. *Biochem. Pharmacol.* 68, 125–134.
- Cookson, M. R., Mead, C., Austwick, S. M., and Pentreath, V. W. (1995). Use of the MTT assay for estimating toxicity in primary astrocyte and C6 glioma cell cultures. *Toxic. In Vitro* 9, 39–48.
- Corcellas, C., Feo, M. L., Torres, J. P., Malm, O., Ocampo-Duque, W., Eljarrat, E., and Barceló, D. (2012). Pyrethroids in human breast milk: Occurrence and nursing daily intake estimation. *Environ. Int.* 47, 17–22.
- Crofton, K. M., and Reiter, L. W. (1984). Effects of two pyrethroid insecticides on motor activity and the acoustic startle response in the rat. *Toxicol. Appl. Pharmacol.* 75, 318–328.
- Crofton, K. M., and Reiter, L. W. (1987). Pyrethroid insecticides and the gamma-aminobutyric acid A receptor complex: Motor activity and the acoustic startle response in the rat. *J. Pharmacol. Exp. Ther.* 243, 946–954.
- Culliford, S. J., Borg, J. J., O'Brien, M. J., and Kozlowski, R. Z. (2004). Differential effects of pyrethroids on volume-sensitive anion and organic osmolyte pathways. *Clin. Exp. Pharmacol. Physiol.* 3, 134–144.
- DeMicco, A., Cooper, K. R., Richardson, J. R., and White, L. A. (2010). Developmental neurotoxicity of pyrethroid insecticides in zebrafish embryos. *Toxicol. Sci.* 113, 177–186.
- Du, G., Shen, O., Sun, H., Fei, J., Lu, C., Song, L., et al. (2010). Assessing hormone receptor activities of pyrethroid insecticides and their metabolites in reporter gene assays. *Toxicol. Sci.* 116, 58–66.
- Eroglu, C., Barres, B. A., and Stevens, B. (2008). Glia as active participants in the development and function of synapses. In *Structural and Functional Organization of the Synapse* (J. W. Ehlers and M. D. Hell, Eds.). Springer, New York, pp 683–714.
- Elstein, K. H., and Zucker, R. M. (1994). Comparison of cellular and nuclear flow cytometric techniques for discriminating apoptotic subpopulations. *Exper. Cell Res.* 211, 322–331.
- Fenech, M. (2002). Chromosomal biomarkers of genomic instability relevant to cancer. *Drug Discov. Today* 15, 1128–1137.
- Fenech, M., Kirsch-Volders, M., Natarajan, A. T., Surrallés, J., Crott, J. W., Parry, J., et al. (2011). Molecular mechanisms of micronucleus, nucleoplasmic bridge and nuclear bud formation in mammalian and human cells. *Mutagenesis* 26, 125–132.
- Food and Drug Administration (FDA). (2015). Pesticide Residue Monitoring. Center for Food Safety and Applied Nutrition. US Department of Health and Human Services. Available at: <http://www.fda.gov/Food/FoodborneIllnessContaminants/Pesticides/UCM2006797.htm>.
- Galluzzi, L., Vitale, I., Abrams, J. M., Alnemri, E. S., Baehrecke, E. H., Blagosklonny, M. V., Dawson, T.M., Dawson, V.L., El-Deiry, W.S., Fulda, S., et al. (2012). Molecular definitions of cell death subroutines: recommendations of the Nomenclature Committee on Cell Death. *Cell Death Differ.* 1, 107–120.
- Go, V., Garey, J., Wolff, M. S., and Pogo, B. G. (1999). Estrogenic potential of certain pyrethroid compounds in the MCF-7 human breast carcinoma cell line. *Environ. Health Persp.* 107, 173–177.
- Gómez, C., Bandez, M. J., and Navarro, A. (2007). Pesticides and impairment of mitochondrial function in relation with the parkinsonian syndrome. *Front. Biosci.* 12, 1079–1093.
- Gonzalez, L. E., Juknat, A. A., Venosa, A. J., Verrengia, N., and Kotler, M. L. (2008). Manganese activates the mitochondrial apoptotic pathway in rat astrocytes by modulating the expression of proteins of the Bcl-2 family. *Neurochem. Int.* 53, 408–415.
- Gorojod, R. M., Alaimo, A., Porte Alcon, S., Pomilio, C., Saravia, F., and Kotler, M. L. (2015). The autophagic-lysosomal pathway determines the fate of glial cells under manganese-induced oxidative stress conditions. *Free Radic. Biol. Med.* 87, 237–251.
- Guizzetti, M., Pathak, S., Giordano, G., and Costa, L. G. (2005). Effect of organophosphorus insecticides and their metabolites on astroglial cell proliferation. *Toxicology* 215, 182–190.
- Gupta, G., Chaitanya, R. K., Golla, M., and Karnati, R. (2013). Allethrin toxicity on human corneal epithelial cells involves mitochondrial pathway mediated apoptosis. *Toxicol. In Vitro* 27, 2242–2248.
- Hales, T. G., and Tyndale, R. F. (1994). Few cell lines with GABAA mRNAs have functional receptors. *J. Neurosci.* 14, 5429–5436.
- Hernández, A. F., Parrón, T., Tsatsakis, A. M., Requena, M., Alarcón, R., and López-Guarnido, O. (2013). Toxic effects of pesticide mixtures at a molecular level: Their relevance to human health. *Toxicology* 307, 136–145.
- Hughes, M. F., Ross, D. G., Starr, J. M., Scollon, E. J., Wolansky, M. J., Crofton, K. M., and DeVito, M. J. (2016). Environmentally relevant pyrethroid mixtures: A study on the correlation of blood and brain concentrations of a mixture of pyrethroid insecticides to motor activity in the rat. *Toxicology* 359–360, 19–28.
- Indo, H. P., Davidson, M., Yen, H. C., Suenaga, S., Tomita, K., Nishii, T., et al. (2007). Evidence of ROS generation by

- mitochondria in cells with impaired electron transport chain and mitochondrial DNA damage. *Mitochondrion* 7, 106–118.
- Izadi, H., Grundy, J. E., and Bose, R. (2012). Evaluation of the benchmark dose for point of departure determination for a variety of chemical classes in applied regulatory settings. *Risk Anal.* 32, 830–835.
- Johnstone, A. F., Strickland, J. D., Crofton, K. M., Gennings, C., and Shafer, T. J. (2016). Effects of an environmentally-relevant mixture of pyrethroid insecticides on spontaneous activity in primary cortical networks on microelectrode arrays. *Neurotoxicology pii: S0161-813X(16)30083-3*. doi: 10.1016/j.neuro.2016.05.005.
- Kim, Y. J., Sah, R. L., Doong, J. Y., and Grodzinsky, A. J. (1988). Fluorometric assay of DNA in cartilage explants using Hoechst 33258. *Anal. Biochem.* 174, 168–176.
- Kojima, H., Matsunaga, K., Kurokawa, E., Ogata, I., and Nishimoto, I. (1988). Calcium influx: An intracellular message of the mitogenic action of insulin-like growth factor-I. *J. Biol. Chem.* 263, 16561–16567.
- Koureas, M., Tsakalof, A., Tsatsakis, A., and Hadjichristodoulou, C. (2012). Systematic review of biomonitoring studies to determine the association between exposure to organophosphorus and pyrethroid insecticides and human health outcomes. *Toxicol. Lett.* 210, 155–168.
- Krieger, R., ed. (2010). *Hayes' Handbook of Pesticide Toxicology*, Vol. 1, 3rd ed. Academic Press, London, UK.
- Labarca, C., and Paigen, K. (1980). A simple, rapid, and sensitive DNA assay procedure. *Anal. Biochem.* 102, 344–352.
- Lee, H. S., Ghetti, A., Pinto-Duarte, A., Wang, X., Dziewczapolski, G., Galimi, F., Huitron-Resendiz, S., Piña-Crespo, J.C., Roberts, A.J., Verma, I.M., et al. (2014). Astrocytes contribute to gamma oscillations and recognition memory. *Proc. Natl. Acad. Sci. U.S.A.* 111, E3343–3352.
- Liu, H., Xu, L., Zhao, M., Liu, W., Zhang, C., and Zhou, S. (2009). Enantiomer-specific, bifenthrin-induced apoptosis mediated by MAPK signalling pathway in Hep G2 cells. *Toxicology* 3, 119–125.
- Livak, K. J., and Schmittgen, T. D. (2001). Analysis of relative gene expression data using real-time quantitative PCR and the 2(- $\Delta\Delta C(T)$ ) method. *Methods* 25, 402–408.
- Malkiewicz, K., Koteras, M., Folkesson, R., Brzezinski, J., Winblad, B., Szutowski, M., and Benedikz, E. (2006). Cypermethrin alters Glial Fibrillary Acidic Protein levels in the rat brain. *Environ. Toxicol. Pharmacol.* 21, 51–55.
- Marshall, S., Gennings, C., Teuschler, L.K., Stork, L.G., Tornerovelez, R., Crofton, K.M., and Rice, G.E. (2013). An empirical approach to sufficient similarity: combining exposure data and mixtures toxicology data. *Risk Anal.* 33(9), 1582–1595.
- Martinou, J. C., and Youle, R. J. (2006). Which came first, the cytochrome c release or the mitochondrial fission?. *Cell Death Differ.* 13, 1291–1295.
- Mattson, M. P., and Kroemer, G. (2003). Mitochondria in cell death: Novel targets for neuroprotection and cardioprotection. *Trends Mol. Med.* 9, 196–205.
- Maurya, S. K., Mishra, J., Abbas, S., and Bandyopadhyay, S. (2016). Cypermethrin stimulates GSK3 $\beta$ -dependent A $\beta$  and p-tau proteins and cognitive loss in young rats: Reduced HB-EGF signaling and downstream neuroinflammation as critical regulators. *Mol. Neurobiol.* 53, 968–982.
- Maurya, S. K., Rai, A., Rai, N. K., Deshpande, S., Jain, R., Mudiham, M. K., et al. (2012). Cypermethrin induces astrocyte apoptosis by the disruption of the autocrine/paracrine mode of epidermal growth factor receptor signaling. *Toxicol. Sci.* 125, 473–487.
- McManus, I. C., Harrison, V., and Mason, O. (2013). Neurobehavioral problems following low-level exposure to organophosphate pesticides: A systematic and meta-analytic review. *Crit. Rev. Toxicol.* 43, 21–44.
- Mense, S. M., Sengupta, A., Lan, C., Zhou, M., Bentsman, G., Volsky, D. J., et al. (2006). The common insecticides cyfluthrin and chlorpyrifos alter the expression of a subset of genes with diverse functions in primary human astrocytes. *Toxicol. Sci.* 93, 125–135.
- Morgan, M. K. (2012). Children's exposures to pyrethroid insecticides at home: A review of data collected in published exposure measurement studies conducted in the United States. *Int. J. Environ. Res. Public Health* 9, 2964–2985.
- Mosmann, T. (1983). Rapid colorimetric assay for cellular growth and survival: Application to proliferation and cytotoxicity assays. *J. Immunol. Methods* 65, 55–63.
- Munson, R., Jr, Westermarck, B., and Glaser, L. (1979). Tetrodotoxin-sensitive sodium channels in normal human fibroblasts and normal human glia-like cells. *Proc. Natl. Acad. Sci. U.S.A.* 76, 6425–6429.
- Narahashi, T. (2000). Neuroreceptors and ion channels as the basis for drug action: Past, present, and future. *J. Pharmacol. Exp. Ther.* 294, 1–26.
- Narahashi, T., Zhao, X., Ikeda, T., Nagata, K., and Yeh, J. Z. (2007). Differential actions of insecticides on target sites: Basis for selective toxicity. *Hum. Exp. Toxicol.* 26, 361–366.
- Natarajan, A., Molnar, P., Sieverdes, K., Jamshidi, A., and Hickman, J. J. (2006). Microelectrode array recordings of cardiac action potentials as a high throughput method to evaluate pesticide toxicity. *Toxicol. In Vitro* 20, 375–381.
- Navarrete, M., and Araque, A. (2014). The Cajalschool and the physiological role of astrocytes: A way of thinking. *Front. Neuroanat.* 19, 33.
- Nishimoto, I., Hata, Y., Ogata, E., and Kojima, I. (1987). Insulin-like growth factor I stimulates calcium influx in competent BALB/c 3T3 cells primed with epidermal growth factor. *J. Biol. Chem.* 262, 12120–12126.
- Nostrandt, A. C., Duncan, J. A., and Padilla, S. (1993). A modified spectrophotometric method appropriate for measuring cholinesterase activity in tissue from carbaryl-treated animals. *Fundam. Appl. Toxicol.* 2, 196–203.
- Osimitz, T. G., and Lake, B. G. (2009). Mode-of-action analysis for induction of rat liver tumors by pyrethrins: Relevance to human cancer risk. *Crit. Rev. Toxicol.* 39, 501–511.
- Patel, S., Pandey, A. K., Bajpayee, M., Parmar, D., and Dhawan, A. (2006). Cypermethrin-induced DNA damage in organs and tissues of the mouse: Evidence from the comet assay. *Mutat. Res.* 607, 176–183.
- Pendergrass, W., Wolf, N., and Poot, M. (2004). Efficacy of MitoTracker Green and CMXRosamine to measure changes in mitochondrial membrane potentials in living cells and tissues. *Cytometry A*. 61, 162–169.
- Pine, M. D., Hiney, J. K., Lee, B., and Dees, W. L. (2008). The pyrethroid pesticide esfenvalerate suppresses the afternoon rise of luteinizing hormone and delays puberty in female rats. *Environ. Health Persp.* 116, 1243–1247.
- Poot, M., Gibson, L. L., and Singer, V. L. (1997). Detection of apoptosis in live cells by MitoTracker Red CMXRos and SYTO dye flow cytometry. *Cytometry* 27, 358–364.
- Posada-Duque, R. A., Palacio-Castañeda, V., and Cardona-Gómez, G. P. (2015). CDK5 knockdown in astrocytes provide neuroprotection as a trophic source via Rac1. *Mol. Cell Neurosci.* 68, 151–166.



- Roma, G. C., Camargo-Mathias, M. I., de Oliveira, P. R., Furquim, K. C., and Bechara, G. H. (2013). Neurotoxic action of permethrin in *Rhipicephalus sanguineus* (Latreille, 1806) (Acari: Ixodidae) female ticks. Morphological and cytochemical evaluation of the central nervous system. *Vet. Parasitol.* **196**, 482–491.
- Romero, A., Ares, I., Ramos, E., Castellano, V., Martínez, M., Martínez-Larrañaga, M. R., Anadón, A., and Martínez, M. A. (2015). Evidence for dose-additive effects of a type II pyrethroid mixture. In vitro assessment. *Environ. Res.* **138**, 58–66.
- Romero, A., Ramos, E., Castellano, V., Martínez, M. A., Ares, I., Martínez, M., Martínez-Larrañaga, M. R., and Anadón, A. (2012). Cytotoxicity induced by deltamethrin and its metabolites in SH-SY5Y cells can be differentially prevented by selected antioxidants. *Toxicol. In Vitro* **26**, 823–830.
- Saftig, P. (2005). Lysosomes. In *History and Morphology of the Lysosome* (R. Lüllmann-Rauch, Ed.), pp. 1–16. *Landes Bioscience/Eurekah.com*. Springer Science and Business Media, New York, NY.
- Shafer, T. J., and Meyer, D. A. (2004). Effects of pyrethroids on voltage-sensitive calcium channels: A critical evaluation of strengths, weaknesses, data needs, and relationship to assessment of cumulative neurotoxicity. *Toxicol. Appl. Pharmacol.* **196**, 303–318.
- Shafer, T. J., Rijal, S. O., and Gross, G. W. (2008). Complete inhibition of spontaneous activity in neuronal networks in vitro by deltamethrin and permethrin. *Neurotoxicology* **29**, 203–212.
- Sheridan, C., and Martin, S. J. (2010). Mitochondrial fission/fusion dynamics and apoptosis. *Mitochondrion* **6**, 640–648.
- Shiraishi, T., Black, K. L., Ikezaki, K., and Becker, D. P. (1991). Peripheral benzodiazepine induces morphological changes and proliferation of mitochondria in glioma cells. *J. Neurosci. Res.* **30**, 463–474.
- Simoniello, M. F., Gigena, F., Poletta, G., Loteste, A., Kleinsorge, E., et al. (2009). Alkaline comet assay for genotoxic effect detection in neotropical fish *Prochilodus lineatus* (Pisces, Curimatidae). *Bull. Environ. Contam. Toxicol.* **83**, 155–158.
- Sims, K. D., Straff, D. J., and Robinson, M. B. (2000). Expression of the EAAC1 subtype of glutamate transporter through activation of phosphatidylinositol 3-kinase. *J. Biol. Chem.* **275**, 5228–5237.
- Singh, A. K., Tiwari, M. N., Dixit, A., Upadhyay, G., Patel, D. K., Singh, D., et al. (2011). Nigrostriatal proteomics of cypermethrin-induced dopaminergic neurodegeneration: Microglial activation-dependent and -independent regulations. *Toxicol. Sci.* **122**, 526–538.
- Soderlund, D. M. (2012). Molecular mechanisms of pyrethroid insecticide neurotoxicity: Recent advances. *Arch. Toxicol.* **2**, 165–181.
- Soderlund, D. M., Clark, J. M., Sheets, L. P., Mullin, L. S., Picirillo, V. J., et al. (2002). Mechanisms of pyrethroid neurotoxicity: Implications for cumulative risk assessment. *Toxicology* **171**, 3–59.
- Sofroniew, M. V., and Vinters, H. V. (2010). Astrocytes: Biology and pathology. *Acta Neuropathol.* **119**, 7–35.
- Sontheimer, H. (1994). Voltage-dependent ion channels in glial cells. *Glia* **11**, 156–172.
- Spencer, C. I., Yuill, K. H., Borg, J. J., Hancox, J. C., and Kozłowski, R. Z. (2001). Actions of pyrethroid insecticides on sodium currents, action potentials and contractile rhythm in isolated mammalian ventricular myocytes and perfused hearts. *J. Pharmacol. Exp. Ther.* **298**, 1067–1082.
- Srivastava, A. K., Srivastava, P. K., Al-Khedhairi, A. A., Musarrat, J., and Shukla, Y. (2012). Allethrin-induced genotoxicity and oxidative stress in Swiss albino mice. *Mutat. Res.* **747**, 22–28.
- Tabarean, I. V., and Narahashi, T. (1998). Potent modulation of tetrodotoxin-sensitive and tetrodotoxin-resistant sodium channels by the type II pyrethroid deltamethrin. *J. Pharmacol. Exp. Ther.* **284**, 958–965.
- Tayebati, S. K., Di Tullio, M. A., Ricci, A., and Amenta, F. (2009). Influence of dermal exposure to the pyrethroid insecticide deltamethrin on rat brain microanatomy and cholinergic/dopaminergic neurochemistry. *Brain Res.* **1301**, 180–188.
- Tsuji, R., Yamada, T., and Kawamura, S. (2012). Mammal toxicology of synthetic pyrethroids. *Top. Curr. Chem.* **314**, 83–111.
- Tulve, N. S., Jones, P. A., Nishioka, M. G., Fortmann, R. C., Croghan, C. W., Zhou, J. Y., Fraser, A., Cave, C., and Friedman, W. et al. (2006). Pesticide measurements from the First National Environmental Health Survey of child care centers using a multi-residue GC/MS analysis method. *Environ. Sci. Technol.* **40**, 6269–6274.
- U.S. Environmental Protection Agency (USEPA). (2002). A review of the reference dose and reference concentration processes. Risk Assessment Forum. EPA/630/P-02/002F, Final Report. Washington, DC.
- Wang, S., Castle, N. A., and Wang, G. K. (1992). Identification of RBK1 potassium channels in C6 astrocytoma cells. *Glia* **5**, 146–153.
- Wätjen, W., Haase, H., Biagioli, M., and Beyersmann, D. (2002). Induction of apoptosis in mammalian cells by cadmium and zinc. *Environ. Health Persp.* **110**, 865–867.
- Weiner, M. L., Nemeč, M., Sheets, L., Sargent, D., and Breckenridge, C. (2009). Comparative functional observational battery study of twelve commercial pyrethroid insecticides in male rats following acute oral exposure. *Neurotoxicology* **30(Suppl.)**, S1–S16.
- WHO (2010). The WHO recommended classification of pesticides by hazard. Guidelines to Classification 2009. International Programme on Chemical Safety, World Health Organization, Geneva. Available at: [http://www.who.int/ipcs/publications/pesticides\\_hazard\\_2009.pdf?ua=1](http://www.who.int/ipcs/publications/pesticides_hazard_2009.pdf?ua=1).
- Wielgomias, B., Nahorski, W., and Czarnowski, W. (2013). Urinary concentrations of pyrethroid metabolites in the convenience sample of an urban population of Northern Poland. *Int. J. Hyg. Environ. Health* **216**, 295–300.
- Wolansky, M. J., Gennings, C., and Crofton, K. M. (2006). Relative potencies for acute effects of pyrethroids on motor function in rats. *Toxicol. Sci.* **89**, 271–277.
- Wolansky, M. J., Gennings, C., DeVito, M. J., and Crofton, K. M. (2009). Evidence for dose additive effects of pyrethroids on motor activity in rats. *Environ. Health Persp.* **117**, 1563–1570.
- Wolansky, M. J., and Harrill, J. A. (2008). Neurobehavioral toxicology of pyrethroid insecticides: A critical review. *Neurotoxicol. Teratol.* **30**, 55–78.
- Wolansky, M. J., McDaniel, K. L., Moser, V. C., and Crofton, K. M. (2007). Influence of dosing volume on the neurotoxicity of bifenthrin. *Neurotoxicol. Teratol.* **3**, 377–384.
- Zeidán-Chuliá, F., Salmina, A. B., Malinovskaya, N. A., Noda, M., Verkhatsky, A., and Moreira, J. C. (2014). The glial perspective of autism spectrum disorders. *Neurosci. Biobehav. Rev.* **38**, 160–172.